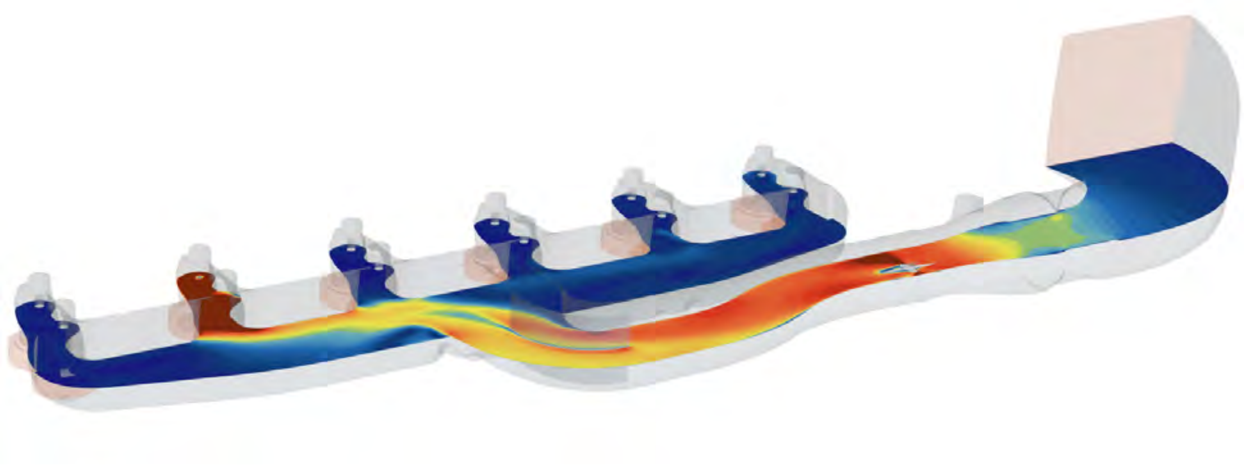

CFD driven design and optimization of a natural gas engine inlet manifold using overset mesh

Optimizing an inlet manifold for Volvo Penta's G17 engine using overset mesh in STAR-CCM+ and designing in Creo Parametric

Master's thesis in Product development and Mobility engineering

Marcin Kryger
Filip Rosén

Department of Mechanics and Maritime Sciences
CHALMERS UNIVERSITY OF TECHNOLOGY
Gothenburg, Sweden 2026
www.chalmers.se

Master's thesis 2026

CFD driven design and optimization of a natural gas engine inlet manifold using overset mesh

Optimizing an inlet manifold for Volvo Penta's
G17 engine using overset mesh in
STAR-CCM+ and designing in Creo Parametric

Marcin Kryger
Filip Rosén

CHALMERS
UNIVERSITY OF TECHNOLOGY

Department of Mechanics and Maritime Sciences
Division of Fluid Dynamics
Chalmers University of Technology
Gothenburg, Sweden 2026

CFD driven design and optimization of a natural gas engine inlet manifold using overset mesh
Optimizing an inlet manifold for Volvo Penta's G17 engine using overset mesh in STAR-CCM+ and designing in Creo Parametric
Marcin Kryger, Filip Rosén

© Marcin Kryger, Filip Rosén, 2026.

Supervisor: Valery Chernoray, Chalmers University of technology
Examiner: Valery Chernoray, Division of Fluid Dynamics

Master's Thesis 2026
Department of Mechanics and Maritime Sciences
Division of Fluid Dynamics
Chalmers University of Technology
SE-412 96 Gothenburg
Telephone +46 31 772 1000

Cover: Flow visualization in STARCCM+ showing the air velocity in a manifold for a six-cylinder engine.

Typeset in LaTeX
Printed by Chalmers Reproservice
Gothenburg, Sweden 2026

CFD driven design and optimization of a natural gas engine inlet manifold using overset mesh
Optimizing an inlet manifold for Volvo Penta's G17 engine using overset mesh in STAR-CCM+ and designing in Creo Parametric
Marcin Kryger, Filip Rosén
Department of Mechanics and Maritime Sciences
Chalmers University of Technology

Abstract

With a constant strive towards sustainability, especially for vehicles, Volvo Penta has committed towards research and development of using renewable fuels to power their engine platforms. One example of a renewable fuel is biogas (bio-methane) which can be used in spark ignition Otto-cycle engines. This is a substitution to one of the most widely used fossil fuels today, which is petrol. For an engine to work properly with high efficiency and minimized environmental impact, the flow of air and fuel entering the engine is of paramount importance. It is crucial to ensure that the air-fuel mixture is delivered to each cylinder with minimal pressure losses and that the distribution of the mixture between the cylinders is equal. One key component affecting this is the intake manifold which is responsible for distributing air from the turbocharger to the six cylinders, and this component was the main focus of the analysis conducted throughout this project. After a thorough background study mapping out which parameters affect intake performance, existing concepts and patents, a design-build-test cycle (DBT) was used including generation of concepts and several evaluations and design-phases. A comprehensive requirements specification was created to use during the development process. Concepts were then designed in Creo Parametric and pre-processed in ANSA. Evaluation of concepts was carried out in STARCCM+ with 3D CFD simulations, both with steady state conditions and with fully transient boundary conditions imported from 1D simulations. A new method for simulating transient valve behaviour was developed using an overset mesh approach, allowing accurate replication of the pulsating gas dynamics within the manifold. The simulation results were used to refine and optimize the secondary duct of the inlet manifold, focusing on minimizing the pressure drop and guaranteeing an equal distribution to all cylinders. The used CFD-evaluation method agrees well with 1D simulation results, showcasing that the more data-efficient overset mesh simulation process is a viable option for future design work. The results also showed promising potential for increasing engine performance through incremental design changes that can be implemented with minimal modifications to the existing manifold-design.

Keywords: biogas, inlet manifold, pressure loss, distribution, design-build-test cycle, CFD, overset mesh, STARCMM+

Acknowledgements

A special thanks to our supervisors Thomas J Larsson and Johan Abrahamsson at Volvo Penta, to all employees at HDEP and CAE as well as consulting expert Daniel Håkansson. We would also like to thank our manager Linda Bodforss, and a special thank you to our supervisor and examiner at Chalmers, Valery Chernorey.

Marcin Kryger, Filip Rosén, Gothenburg, May, 2026

List of Acronyms

Below is the list of acronyms that have been used throughout this thesis:

CFD	Computational Fluid Dynamics
CAD	Computer Aided Design
SI	Spark Ignition
CI	Compression Ignition
TC	Top - Center
BC	Bottom - Center
BMEP	Brake Mean Effective Pressure
cv	coefficient of variation

Contents

List of Figures

List of Tables

1

Introduction

Internal combustion engines are vital in today's society. They help powering transportation in land, sea and air and supply energy production that powers our modern world. This is thanks to their high power- to weight ratio, low cost and simplicity. In 1860 the technology with internal combustion engines became a reality, before the dominating principle was the steam engine [3].

J. J. E. Lenoir was one of the first people to develop an engine that used a gas- and air mixture at atmospheric pressure. During the first half of the piston stroke, gas and air was drawn into the cylinder which was ignited with a spark. Then during the second half, the pressure from the ignited air-gas mixture powered the piston and finished with releasing the exhausts. This engine had an efficiency of 5% [3].

Then in 1876 Nicolaus A. Otto presented a four stroke piston engine after he also worked with an atmospheric engine that had an efficiency of 11%. The strokes were intake, compression, ignition where expansion powered the crankshaft and lastly the exhaust releasing the resulting gases. This revolutionized the engine industry with its largely reduced weight and volume which paved the way for how engines are made today [3].

According to the Environmental Protection Agency, the production of heat and electricity was accountable for 34% of the global greenhouse emissions the year 2019. This is because of burning fossil fuels such as coal, oil and natural gas [4]. The need for improvements of efficiency in internal combustion engines is created by the uncertainty in long-term availability of petroleum-based fuels which are non-renewable. This drives manufacturers to look into fuels without petroleum such as ethanol, biodiesel and natural gas [3].

1.1 Background

Sustainability is a core value for a company like Volvo Penta. This has resulted in increased research and development into using renewable fuels to power their engine platforms. Biogas (bio-methane) is one example of a renewable fuel that can be used in spark ignition Otto-cycle engines. This is a substitution to petrol which is one of the most widely used fossil fuels today. High efficiency and minimized environmental impact are crucial parameters for an engine. Minimal pressure losses and that the distribution of air-fuel mixture between the cylinders is equal are therefore important aspects [3]. The main component responsible for this is the intake manifold that delivers air from the turbocharger to the six cylinders.

1.2 Volvo Penta

Volvo Penta is part of Volvo Group, and they specialises in delivering powertrains for land and marine applications. They have a wide variety of customers such as construction, agriculture, yachts and forestry. They also produce engines for power generation, so-called gen-set technology which is used as backup power in hospitals, producing electricity where there is no power-grid and for energy storages [5].

With an increased need for energy production, for example data centres and powering construction sites along with crucial backup energy for hospitals, demands are made on what energy sources are used to power these. Volvo Penta has a wide variety of diesel engines for gen-set technology, but they have recently announced an engine that is powered with natural gas to use in combination with existing infrastructure. Natural gas emits about 25% less carbon dioxide than that of diesel and gasoline which makes it an alternative fuel [3]. The engine can also run on bio-methane which can be considered fully renewable.

1.3 Purpose & goal

The purpose of the thesis is to optimize the flow and distribution of the air-fuel mixture between the cylinders in a natural gas - powered engine. More specifically Volvo Penta's G17 natural gas engine. The focus lies in the flow of gas to the cylinders trough the intake manifold in order to be able to improve engine parameters such as efficiency, environmental impact and the possibility to use renewable fuel sources such as biogas.

The goal is to design a manifold that grants lower pressure losses than the current design, while ensuring a more even distribution of the air-fuel mixture between the cylinders than what is currently achieved.

Ecological aspects that are to be considered in this project is the purpose of the engine to run on renewable fuels such as bio-methane. There is also the fact that improved engine efficiency can also reduce environmental impact on the engines that run on non-renewable energy sources such as diesel or petrol.

One ethical aspect is the confidentiality, to keep certain aspects of the project confidential in order to maintain fair competition and protect company intellectual property. This aspect is managed trough a signed non-disclosure-agreement and mandatory education on data awareness and other safety aspects such as physical safety. Another ethical concern is sensitive personal data. Sensitive data that Volvo Penta has stored is used with respect and concern following GDPR to ensure customer integrity.

This project is not directly affecting social aspects in broader society, but an argument can be made that a more emission free environment with renewable energy sources can positively affect for example peoples well-being. One social aspect however that is directly relevant for the project is the collaboration between students and employees, where the students adhere to the company's code of conduct.

The use of AI during this project is used as a supporting tool to help with for example grammar or report formality, or with inspiration for potential solutions. For these purposes, Volvo Group's internal model was used to maintain data integrity. The ideas, designs and the work presented in this project are entirely produced by the authors.

1.4 De-limitations

Because of the time constraint of 5 months the scope of the project is adjusted accordingly. The number of design iterations heavily depends on the amount of time that is spent at the design-phase of the thesis work.

While there are many crucial parts, systems and concepts interacting inside an engine, this project only focuses on the intake manifold which is part of the airflow system. So the focus of this project is from the intercooler to the inlet ports into the cylinders, which is the high pressure part of the system. Exactly what parts this applies on is presented under section 2.2 in Figure 2.3.

The project does not focus on the structural aspect of the manifold, for example no finite element analysis is done to make sure it can withstand the pressure cycles it is subjected to. Neither is the material or any aesthetic aspects such as color of the manifold of consideration, only the performance of airflow is the focus.

Another de-limitation is that the manufacturing and installation is only to be considered with the methods that are used today, therefore no new manufacturing method is explored. Cost is also only considered as an aspect in the discussion of the results, meaning no thorough cost-calculations will be done.

1.5 Research questions

The following research questions are to be investigated in this thesis:

- Which aspects and parameters are important to consider when improving the airflow to the engine?
- How can an intake manifold be designed to increase engine performance with the given constraints and requirements?
- How can a simulation method using overset mesh be implemented to simulate valve behaviour and unsteady flow?

2

Theory

In the following chapter, relevant background theory is presented along with figures and equations to ease reading of the report.

2.1 Internal combustion

The type of an internal combustion engine is amongst other parameters classified by the cycle that is used. Two common such cycles that are found in a wide range of applications today are the Otto (SI) and Diesel (CI) cycles [3].

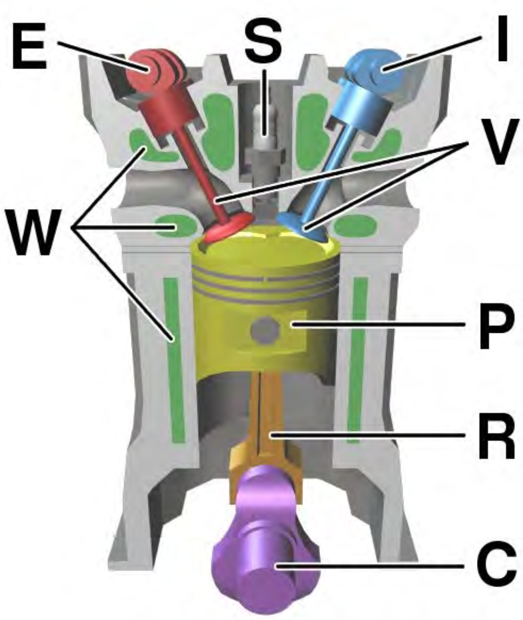

Figure 2.1: Parts of a reciprocating engine. [1], CC BY-SA 3.0

As mentioned in chapter 1, introduced in practice by Nicolaus A. Otto, the Otto cycle is a 4-stroke engine cycle designed for reciprocating piston engines, consisting of "a compression stroke before ignition, an expansion or power stroke where work was delivered to the crankshaft, and finally an exhaust stroke" [3]. A cutaway representation of a reciprocating 4-stroke piston engine can be seen in Figure 2.1, where C denotes the crankshaft, R the connecting rod and P the piston. In a reciprocating engine "each piston moves back and forth in a cylinder and transmits power from the high-pressure and temperature burned gases inside the cylinder through the piston and the connecting rod and crank mechanism ", enabling the extraction of rotating motion from the process of burning a fuel. The crankshaft rotation causes the piston to move in a "cyclical" motion, where the upper position is denoted as top-center (TC) and bottom position is denoted as bottom-center (BC) [3].

In an SI engine, it is crucial that the fuel is "well mixed with the air inducted into the cylinder" to facilitate proper combustion [3]. This is especially important because this engine cycle relies on a pre-mixed blend of combustible gases in order for combustion to take place.

The cylinder to cylinder variations in the combustible charge are "important" and determine the engine behaviour, affecting the smoothness and reliability of the engine operation. Differences in the burning rate of the air-fuel mixture are affected by several factors, but one that is crucial is the variation of the quantities of fuel and air supplied to each cylinder each cycle. Formation of emissions within each cylinder is also closely related to how the combustion process occurs, meaning they are also affected by how fuel and air are distributed in multi-cylinder engines [3].

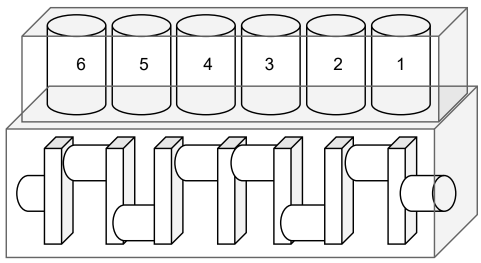

Figure 2.2: Schematic of in-line 6 cylinder engine, with cylinder numbering

Another parameter that is used to classify an engine is the number of cylinders it has, engines with more than one cylinder are called multi-cylinder engines. The cylinders can be placed in different arrangements, for example In-line where the cylinders are aligned in a straight line, V-engine where the cylinders are placed in a V-shape and another one where the cylinders are placed radially. An engine is denoted with how many cylinders it has and what their arrangement is, for example a six cylinder engine with a In-line configuration is called an "In-line six" or "straight six" and can be seen in Figure 2.2. It is also common to denote it with the size of the volume, for example "3,6 liter In-line six" [3].

The firing sequence or order is another important parameter of an engine, it describes which spark at which cylinder ignites and causes the power stroke. The firing sequence for an In-line 4 cylinder engine is 1,2,4,3 or 1,3,4,2 where the number denotes what cylinder that is being ignited [3]. It can be displayed with for example the angle of the crankshaft to see what cylinder fires at what time, to see which firing sequences that overlap for example.

Turbocharging is used to increase the amount of air that's available during the combustion process. This makes it possible to extract more power from the same engine size, also allowing the engine to reach a higher efficiency. This compressor process utilizes the energy from the exhaust gases to spin a turbine that drives the compressor, using energy that would otherwise go to waste. The compressed air from the turbocharger can be passed through an intercooler, which cools the charge further increasing density, maximizing the mass of air that can be forced into the engine [3].

2.1.1 Alternative fuels

Another crucial parameter that defines the type of engine is the fuel type and mixture preparation method used. Historically, SI combustion engines have been fuelled through a carburettor which was responsible for both metering and vaporizing of liquid fuels, such as gasoline [3].

Natural gas is an alternative fuel that can be used in boosted SI engines. Methane, making up most of the composition, has comparable characteristics to those of gasoline. It allows for a reduction in CO_2 emissions, as the gas exhibits a higher molar hydrogen:carbon ratio, meaning that when burned the CO_2 emissions on complete combustion are lower than those of gasoline and diesel by about 25% [3].

One method of metering the natural gas into the intake air is through a low-pressure regulator. Because the fuel is gaseous, it is easier to get a proper air-fuel mixture than with gasoline as no evaporation of fuel droplets is involved [3].

2.1.2 Air Induction

The quantity of air that is present in the combustion chamber at the onset of burn initiation directly limits the amount of fuel that can be combusted. This makes the engine's "breathing capacity" a crucial design objective, directly affecting the torque and subsequently power that the engine produces [3].

The intake system in an SI engine is also a crucial part of the mixture preparation process. Firstly, an important goal is to ensure that fuel and air are mixed sufficiently, but another goal is also to ensure an even charge distribution between the cylinders of the engine [3]. This was as mentioned in section 2.1 instrumental in the process of controlling the behaviour of the combustion and formation of emissions.

A key metric used to describe how well the air induction system functions is the volumetric efficiency η_V. According to [3] this measure is primarily used in naturally aspirated (non-turbocharged) engines, and is expressed in Equation 2.1.

$$\eta_V = \frac{m_a}{\rho_{a_0} V_d} \tag{2.1}$$

The parameter m_a describes the mass of air that has been trapped within the cylinder volume, where the swept (defined by the piston movement) displacement volume is denoted V_d. Air density is described by $\rho_{a,0}$, and commonly refers to ambient or atmospheric conditions. Another similar definition expressed by [6] is defined by the mass of air trapped in the cylinder divided by the mass of air contained in swept volume of the cylinder at inlet manifold density. Its validity to use for turbocharged engines depends on what reference condition of air density is used. If the density of air in the inlet manifold is used, the formula could also be applied to describe turbocharged engines, as it accounts for the higher pressure of the intake charge.

2.1.3 Knock/autoignition

Knock is a phenomenon that occurs when the air/fuel mixture ignites unevenly or prematurely before the piston is at TDC in an SI engine. For example, a "pocket" of air/fuel mixture is ignited prematurely before the rest of the mixture is ignited, through for example a hot surface. This could lead to damage on the piston because of the shock-wave that is created or the high temperature that could melt the top of the piston for example. The high temperature wears the engine and increases the risk of even more knocking. The spark-plug can also be damaged by the shock-wave [3].

2.2 Volvo Penta’s G17 engine

The G17 engine from Volvo Penta is built on the diesel-engine D17, it is meant to help them transition to a more decarbonized future by using natural gas. It is a 17-liter In-line 6 cylinder engine, built to run on conventional natural gas, renewable, and pipe-line quality natural gas by connecting directly to existing gas infrastructure [2]. A summary of relevant specifications are displayed in table 2.1.

Table 2.1: Specifications of Volvo Pentas G17 engine. [2]

Fuel type	Natural gas
Cylinders	6
Volume	17,26 liter
Prime power	554 kVA
Speed	1500/1800 rpm
Firing sequence	1,5,3,6,2,4

There are different ways to measure the power in specifically a power generating engine. One unit is kVA which is kilovolt ampere, another one is kWm which stands for kilowatt mechanical effect on the axle and kWe which is the electrical effect delivered in kilowatts. The engines prime power is given at 60hz, which means operating at a speed of 1800 rpm. It is also possible to operate it at 50hz, with a speed of 1500 rpm. The prime power is an ISO standard of an engines ability to supply power at 70% load for an unlimited number of hours. The G17 has the same amount of cylinders, same displacement volume and firing sequence as the D17. A visual representation of the G17 engine is presented in Figure 2.3 below along with red lines marking the design limitations and arrows explaining different parts of the manifold. The arrow pointing to cylinder one indicates the order of the cylinders. The plenum is the dark brown part that is fit to the engine block encapsulating the inlet ports inside the engine. The plenum connects in the middle of it with the secondary pipe. Before the secondary pipe is a throttle regulating the amount of air/mixture that is passed through when the air arrives from the intercooler.

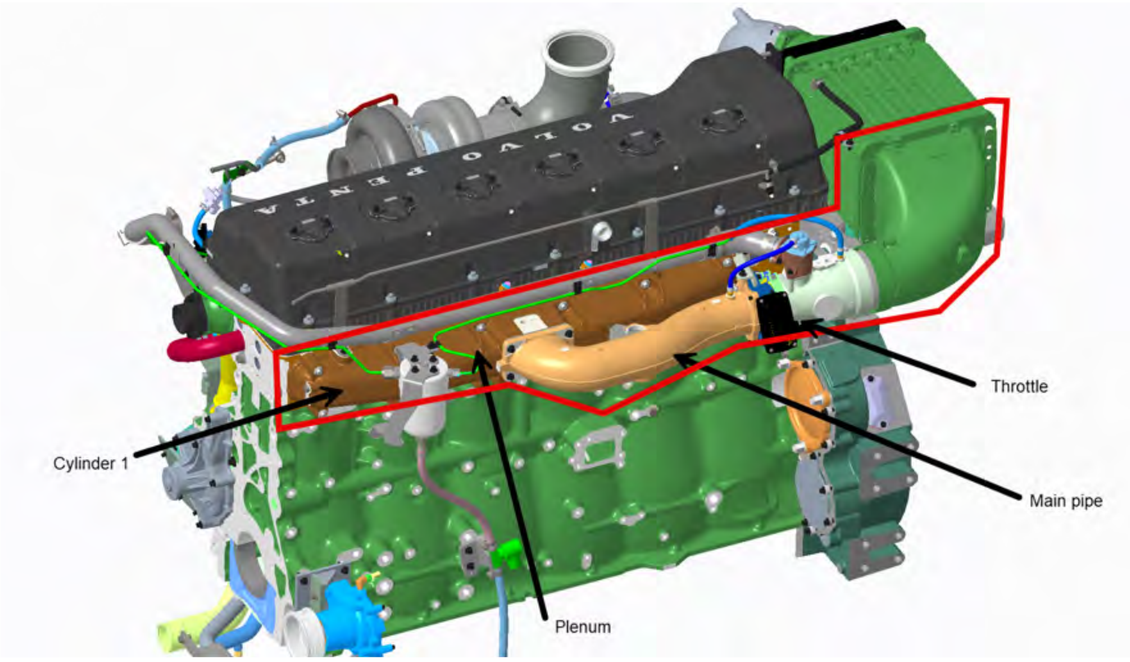

Figure 2.3: G17, with the red line marking the design limitation and black arrows describe the different parts of the engine.

2.3 Manifold tuning

With the design goal of allowing as much air as possible to enter the engine, designing of an intake manifold requires to take various parameters into consideration. Due to friction within the flow, the pressure of the charge stream decreases throughout the manifold. Throughout the process of induction, pressure losses occur as the charge passes the various components comprising the intake system. The pressure drop in the system depends on the charge density, the cross-sectional area where the charge moves through, the engine speed and what the flow resistance is for the elements in the system [3].

As mentioned in subsection 2.1.2 the volumetric efficiency is a key aspect of an engines performance. The mean effective pressure is directly proportional to the volumetric efficiency if all other parameters are unchanged. If the air:fuel ratio is constant, any increase in volumetric efficiency will lead to an increase in the break mean effective pressure (BMEP) which will increase the torque generated. More specifically, the pressure in the manifold when the piston is at BC just before the inlet valve closes has the strongest effect on the volumetric efficiency, other pressure pulses in the inlet period have a smaller impact [6].

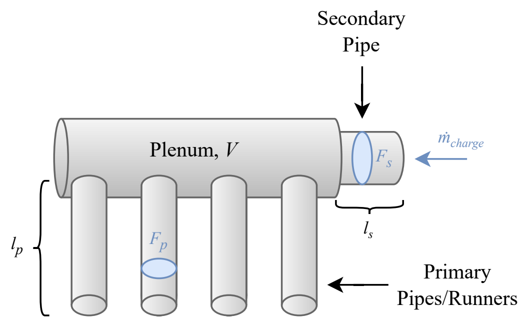

Figure 2.4: Typical plenum arrangement for a 4 cylinder engine

There are two predominant types of pulse resonance modes observed in intake manifolds such as the one seen in Figure 2.4, which affect the volumetric efficiency in different ranges of the engine's operating speed. A visual explanation of the variables can also be seen in Figure 2.4, where l_p and l_s define the lengths of the primary and secondary pipes respectively, V denotes the volume of the plenum chamber, with F_p and F_s representing the cross-sectional area of the primary and secondary runners respectively. The variable n_c describes the number of cylinders. The natural frequencies ω of the resonance in the intake manifold are modelled and expressed by Equation 2.2 and Equation 2.3. The shorter formula expressed in Equation 2.2 describes a resonance that occurs within the individual inlet pipes, also known as intake runners. This is a shorter period oscillation that is predominant at higher engine speeds. The longer period oscillation expressed by Equation 2.3 is caused by the entire manifold volume being at resonance, both the inlet runners and the plenum resonating simultaneously. This second resonance mode is present in the lower range of engine operating speeds [6].

$$\cos \frac{\omega l_p}{a} = 0 \tag{2.2}$$

$$\frac{F_s}{F_p} \cot \frac{\omega l_s}{a} = \frac{\omega V}{F_p a} + n_c \tan \frac{\omega l_p}{a} \tag{2.3}$$

The effect of the manifold on volumetric efficiency is very much dependent on the engine speed because the frequency of the pulses entering the manifold is driven by valve opening and closing events and the movement of the pistons. This shows that it is possible to tune the manifold to give it specific characteristics at different engine speeds [6].

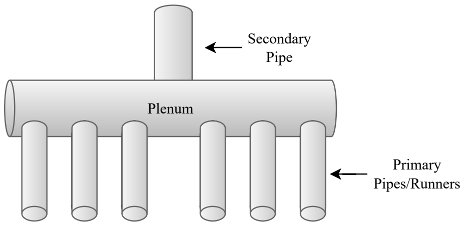

Figure 2.5: Single plenum configuration for in-line 6 engine

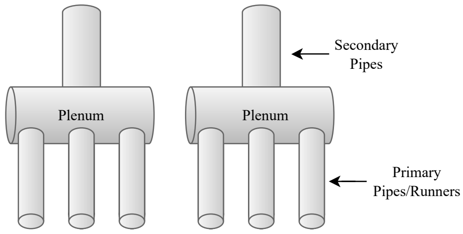

Figure 2.6: Dual plenum configuration for in-line 6 engine

Engine configuration also has a profound role in determining the characteristics of the pulses in the intake manifold. In in-line 4 cylinder engines the two oscillation modes are clearly visible when pairing the engine with a single plenum connected to individual runners. However, two separate plenums like in Figure 2.6 are required for a six-cylinder engine to get a low-speed peak of the volumetric efficiency. Evident in simulation testing an in-line 6 cylinder engine paired with a single plenum manifold as in Figure 2.5 only experienced the short period resonance mode expressed in Equation 2.2, but by dividing the plenum for the six-cylinder into two separate ones, the low-speed peak was regained for the six-cylinder. This phenomena is caused by overlap of the intake pulses in a six-cylinder engine compared to a four-cylinder one. With the cylinders whose induction period does not overlap grouped together in an individual plenum, full advantage can be taken from low-speed resonance. In this case, the secondary pipe is considered to be the flow-path connecting the individual plenums together at their confluence point [6].

2.4 Flow within tubes and channels

A common element that comprises engine intake manifolds is the tube or circular channel, therefore describing the flow within these elements is an important part of characterizing the behaviour of the entire system.

The main portion of pressure losses that occur in the bends of a tube-channel system happen at the inner wall of the bend curvature, where eddies form as the flow separates from the inner wall [7]. This phenomena greatly reduces the cross-section of the main stream and effectively creates a smaller area that the flow can pass through. This loss can be most significantly reduced through an increase of the inner bend radius, or the addition of a circular fairing on the inside corner.

Another method of decreasing a bends flow resistance is the addition of guide-vanes that direct the flow and guide it throughout the bend. This method can have the benefit of not altering the outer dimensions of the geometry, allowing for more compact designs. The vanes can be given an aerodynamic shape, much like an airfoil, and have the biggest potential of improving the flow when placed closer to the inner bend, where the separation occurs [7].

2.5 Computational fluid dynamics

Computational fluid dynamics (CFD) is a tool for analyzing performance and flow in a design of for example some sort of equipment or process. It is possible to get a detailed analysis of the heat- and mass transfer in a flow. There are different types of flow that can be simulated, for example laminar, turbulent and single-phase flow. Single-phase flow is focused on in this project, which involves either a gas or a liquid, in contrast to multiphase flow where there are at least two different phases, for example a mixture of gas and liquid[8].

Navier-Stokes equations can be used to describe turbulent flow and there exist methods for computing more complex CFD problems that use Navier-Stokes equations. An example of that are flows with turbulence fluctuations which are done with Reynolds averaged Navier-Stokes (RANS) methods. With these methods, the fluctuations are averaged and most phenomena are resolved while even more complex problems require additional models to accurately capture all relevant phenomena [8].

The typical workflow when applying CFD to a problem in a design process is the following; geometry modelling, grid generation, defining models, set properties, set boundary and inlet conditions, solve and then analyze the results. First modelling the geometry in a 2D or 3D software with a CAD-program, the model is then imported into a grid generating program where a mesh is applied to the model. This is done to prepare the CFD program to be able to compute correct numerical solutions of the equations from the computational volume. The geometry is in other words "divided into small computational cells". Then the appropriate model for computing is selected, either an already existing one or, if needed, it is possible to create a new one in a programming language such as C. There are several parameters that have to be set for every model, and usually the best choice are the default parameters [8].

After the correct models are chosen, the properties of the fluid are defined. For example its temperature, density and composition. After that all initial boundary conditions are set, inlet, outlet and conditions at the walls, along with other conditions such as periodic boundary conditions. The problem is afterwards solved with a chosen solver, whether that is steady state or transient is determined, and an iteration method is also chosen. Convergence criteria is also decided, which determine when the quality of the results from the simulation are considered satisfactory. Finally the results are evaluated based on the convergence criteria and qualities such as whether the grid size significantly affects the results. Furthermore, the boundary conditions are evaluated along with what turbulence model has been chosen, to evaluate if they are relevant and how much the result depends on these conditions [8]. In a transient simulation, a time step denotes how much the simulation advances through physical time.

The simulated flow can be split up into different sub-layers. In the innermost layer of the mesh closest to the wall, the layer is called the viscous sub-layer, where the flow is almost laminar, here the viscous stresses are dominant. While further away from both the innermost layer and the wall, the sub-layer is called the fully turbulent sub-layer. Here the viscous effect are negligible and the turbulent stresses become dominant. Closer to the wall there is fluctuations in the velocity because of viscous damping and at the wall there is stress on the flow in terms of pure viscous shear. Here, $y+$ is a dimension-less variable that is used to explain the physical extent of the different sub-layers in the flow [8].

2.6 Overset mesh

Overset mesh is a method for setting up different regions inside the simulation software. It is especially useful when simulating cases of mesh interactions and motion, for example when simulating the opening and closing of the valves inside an engine. The principle is that two different meshes are set up, one background mesh and one overset mesh. Then the governing flow equations, which are for example Navier-stokes equations, are computed on both the background mesh and the overset mesh. The cells in the background mesh that overlap with the overset mesh are cut away and then the cell values at the boundary between the overset and the background are interpolated. The same happens with the overset mesh. This produces three cell types, the inactive cut out cells, and then the interpolated cells of both the background and the overset meshes which alternate between donor and acceptor cells. So for each timestep, a cell is either calculated as a regular cell, interpolated or not calculated. Where the donor cells to the background domain are from the overset domain, and vice versa for the donor cells for the overset domain [9]. More on how the overset method works is presented under subsection 3.7.1. This entire process requires no re-meshing, opening the possibility for faster computation.

2.7 Previous Studies

The design of optimized inlet manifold systems is a task that has been undertaken by many engineers throughout history, and one that has also been a central part of past Formula Student SAE competitions. Methods, results and considerations from a range of relevant studies are compiled in this section.

A study of an in-line 6 diesel engine intake manifold was conducted by [10] where aspects such as exit flow velocity, manifold air flow velocity and the turbulence kinetic energy were investigated. The manifold investigated was of the double-plenum configuration as seen in Figure 2.6 at an operating speed of 1600 RPM, where the suggested improved design featured increased primary runner length and a decreased distance between the runner entrances. The study was conducted using a steady-state 3-dimensional CFD analysis with $k - \epsilon$ turbulence modelling. This approach involved simulating one flow-path within the manifold at a time, having one of the outlet ports open and the other ones covered replicating a single open valve.

In the work conducted by [11] the effects of manifold plenum volume on the cyclic variability of combustion in an SI engine were studied. This study involved an experimental setup where the volume of the tested plenum was varied between runs, allowing the observation of its effects on hydro-carbon emissions, brake torque and COV_{imep}, a measure of the cyclic variability. Increasing the volume produced a "pronounced" increase in the brake torque and related measures, as well as a decrease in the hydrocarbon emission and cyclic variability.

2.8 Product development methodology

There are several product development processes that can be used when designing products, it can differ depending if it is a physical product, a digital product or a whole system. Under this section, the process used in this project is described along with different types of product development projects.

2.8.1 The product development process

The process used in this work is similar to a typical product development process. The steps relevant for this work is planning, concept development, system-level design, detail design and testing and refinement. One step that is disregarded is production ramp-up because this is not within the scope of the project. Planning was done in January before the project was started but also at Volvo Penta before the project was initiated and put out as a master thesis. The planning contains involvement with management and corporate strategy along with product planning if it aligns with the company strategy etc. The output from the planning is for example constraints, business goals and key assumptions [12].

Concept development is the most relevant step for this project as it is its main objective. It consists of for example identifying customer needs, establish specifications, concept generation, concept selection, concept testing, setting final specifications, benchmarking of competitive products and modeling and prototyping. During concept generation the goal is to explore ways to address the customer needs and it usually results with 10 to 20 possible concepts where each has a description and a rough sketch. Then the concepts are analyze and sequentially screened down to the most promising ones. It can involve several iterations of generating new concepts and evaluating them. Tools that can be used here are matrices such as pugh- and kesselring matrix. After evaluation the concepts are tested to validate if it customer needs has been met, the market potential of the product and what needs to be improved during further development. Here, simulation tools such as Star ccm+ can be used to see if the customer needs and requirements has been met. Benchmarking of competitor products can help with the product design process by providing ideas and also see how the product aligns with the market demand and customers. Every step of the concept development process can include prototyping and modeling, in this project the modeling consists of sketching by hand and designing in cad. This helps to visualize certain solutions and for example the feasibility of the concepts. An economic analysis is during the development process is crucial for the product the be competitive on the market. As mentioned in the limitations, the economic factor will be taken into consideration but it's not the most important aspect [12].

After the development comes the system-level design were decomposition of the product into components and preliminary design of key concepts are included. Then the detail design which includes complete specification, materials and what standard parts to be purchased from supplier among other things. This also includes for example documentation on how each part is to be produced and the production supply chain for the factory. Here the final decisions on materials selection, robust performance and production cost are made. Testing and refinement is the last step that is relevant to this project, it includes earlier (alpha) prototypes with similar parts as the final product and later (beta) prototypes with the parts from the intended production processes. These are final prototypes which are used by customers and internally in the company to evaluate the products performance and reliability to identify possible changes in the design by engineers [12].

One example of where the design-build-test (DBT) cycle can be implemented in this project is after the system-level design. The iterative cycle can be resembled with the build-measure-learn cycle that Eric Ries mentions in his book "The lean startup" [13]. They are both iterative processes that includes (designing) building a prototype, testing it and collecting measurements and data from it, and then learning from it to then build an improved version. Another common step in the design-build-test cycle is learn which comes after test which is the same as in Ries's terminology, it's abbreviation is DBTL. Build describes the action were a product is built, in most cases its a prototype or a minimum viable product (MVP), this is the same as in DBT. In DBT there is also an emphasis on the actual designing of the product which is the design step before the build step, which is more relevant to this design-project. Measure is the same as test in DBT, were the built prototype is tested and data is collected. This can go different ways, for example, with an MVP its crucial to get feedback as soon as possible on the product to be able to iterate and build an improved product. After this is where learn comes in, with the results from testing the product is re-designed with feedback from either customers or with data from testing which can be for example simulation [13].

2.8.2 Types of product development projects

Within product development there are different types of product development projects that a company can put money and resources on, depending on what aligns with their goals and company strategy. Henderson et. al mentions three types which are incremental, modular and radical project/innovation [14]. Henderson also mentions a fourth one which is architectural innovation but in this project the three main types are incremental, modular and radical. Incremental innovation is about refining and extending an already established design, this could for example be a facelift of a car. This means that no completely new technology or big design-changes has been introduced. Radical innovation means that there is a completely new dominant design and usually with some completely new technology introduced. Modular innovation describes projects that changes a product design concept but the product architecture-how a products' components interact with each other, remains the same. Different from radical innovation that introduces a completely new product architecture. Modular innovation can also be compared with platform innovation where a whole new architecture is created but the design remains fairly the same. So the relation can be that a platform is created with a modular architecture with interchangeable parts but the design remains the same.

3
Method

This project followed a product development process with a design-build-test approach, a flow-chart of this can be seen in figure 3.1 below. It started with a thorough literature review to fill the knowledge gaps to be able to use this knowledge when designing and optimizing the inlet manifold. As well so that the reader had all the background knowledge to be able to read the report. Also research about the topic along with a patent search and analysis of current designs was conducted to establish requirements and constraints. Then during the concept stage which consisted of concept generation, evaluation and screening of concepts was done based on the requirements and constraints. Here brainstorming was used but also generative design was explored with for example a topology optimization as a tool during the concept generation. After the first screening process the remaining concepts were designed in CAD and simulated, in 3D using the CFD program STAR-CCM+. The boundary conditions for the simulation was taken from 1D simulations in GT-Power. This was an iterative process with re-design and simulation to reach the final design. Lastly a prototype of the final concept was printed out using a 3D-printer. All results gathered from the literature study are presented in chapter 4.

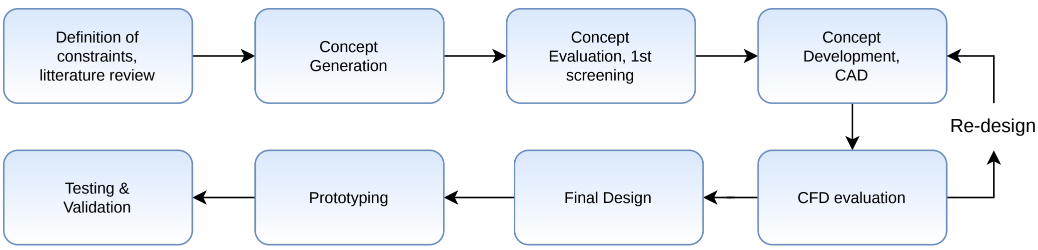

Figure 3.1: The product development process during the project

3.1 Literature review

The results from the literature review are presented both in the theory and results.

3.1.1 Means of information for the literature review

The literature review was done by searching for articles and available books at Chalmers and Volvo Penta. The used databases were for example Chalmers library and Google scholar to find suited and legitimate sources of information. Discovered sources here were articles from for example conferences, previous master thesis's and available books. Books, internal reports and know-how from employees at Volvo Penta were also gathered through meetings for instance.

The existing G17 engine by Volvo Penta was studied both physically and through specification sheets. Facts about it are presented under section 2.2. With this information, requirements and constraints were established that could be used during the design phase. As well as test data from the test-department was analysed to better understand how it was working and possible improvements.

3.1.2 Competitor/market analysis

A competitor and market analysis was made to find inspiration for ideas for the concept generation and see what was available on the market today. Along with a patent search to check what solutions that are under a patent so that the final design don't risk of intruding on any, but also to get design-inspiration.

Information from competitors was gathered through visiting websites and accessing product catalogues and data sheets about the different products that competitors were offering.

Espacenet and google patents were used here to find relevant patents. In Espacenet a classification search was used along with search words. Different combination of classifications, search words and other filters such as year was used to find different patents. One example of classification that was used was "Engines characterized by positive ignition" to narrow down the search. The filtered years was kept untouched since the combustion engine has been in production since the late 1800's. The number of search results were filtered down with classification and then the most relevant patents were picked, based on type of solution, publication year and relevance to G17. One patent for each type of general solution was chosen, for example one patent for solutions using equal length runners.

3.1.3 Analysis of the G17 engine

The previous engine and its manifold was studied to determine possible areas of improvement, this information acted as a foundation for the concept generation stage. The analysis of the G17 engine began with visual inspection of the CAD-design in Creo Parametric. The different parts of the manifold were identified and the parts considered within the design space were isolated. These subsets of components are also mentioned in delimitations regarding which parts are involved in the optimization. Subsequently, the product sheet that is distributed out to the customers was reviewed. It presented key metrics describing different subsystems within the engine, for example rated power at given rpm points.

Prior to the start of this thesis, earlier simulations were also conducted during the development of the existing manifold and they were presented in a report that was also studied. Specifically the simulation method, the mesh and what boundary conditions that were used were studied.

3.2 Production of the requirements and constraints

From all knowledge and information found in the literature review, requirements and constraints were produced that would be the foundation of the design of the manifold. It was done by selecting the most important attributes and characteristics of the manifold, then a table was created with all these. The table was described with a requirement number, then attribute/description of the requirement, the value (how it is measured). Then if it is a requirement, a desire or if it's optional, and after that a justification, what evaluation method to check if it is met and lastly what reference that is used for evaluation. The requirements are not listed in order, rather each requirement is listed in the way they were added. This table was only used when generating the concepts, while it was later used to develop the criteria for the evaluation for the concept with pugh-matrices.

3.3 Inlet manifold concept phase

This section will go through how the different concepts were generated and evaluated.

3.3.1 Concept generation

One tool that was used frequently was brainstorming during the concept generation. There were different brainstorming sessions with sketching to get a quick visualization on different concepts. Some smaller occasions were during the lunch break for example, and during meetings with employees where more general concepts and design techniques were covered. The main brainstorming session was done on the third of march. This was a thorough session where whole concepts were created, these were categorized into the three different types of products mentioned before. During the brainstorming, a whiteboard was used to draw up the different concepts to be able to describe what the idea was and what it looked like. All ideas were welcome and no ideas were disregarded until the concept evaluation phase to encourage innovation. For each concept, a short description along with each sketch was created to present in results but also to be used as a communication tool to be able to keep track of the different concepts. In addition, the concepts were given working names that are not final product names but rather to keep track of them during the design phase.

3.3.2 Usage of AI (Generative design)

A method with generative design was tried to optimize the manifold. A large volume which was the design space given in the requirements was optimized using a cost function and re-mesh. Even though it gave a lot of knowledge and experience with STAR-CCM+ this gave no results worth showing.

3.3.3 Concept evaluation-first screening process

This section presents how the concept evaluation was carried out. This first screening was done with Pugh-matrices. The criteria in the matrix was based on the requirements and constraints, for example size and manufacturability. Pressure drop and air distribution are the main objectives and therefore they are criteria. As well as other criteria such as complexity that was learned during the generation phase that it was an important aspect. So the requirements and constraints table is a more thorough in-depth explanation of the requirements. While the criteria used in the Pugh matrices were made to be easier to use for evaluation, they are based on those requirements. In the Pugh-matrix all 9 concepts were listed and the existing manifold, along with 7 different criteria. Then a concept was selected to act as reference during the evaluation, then a comparison was made between each concept and the reference concept. If the compared concept performed better than the reference, it received a "+", if it performed worse it got a "-", and if it was deemed as good as the reference it got a zero. During this comparison the description and sketches were used and to prevent bias towards any of the concepts, each comparison was thoroughly discussed and if there was uncertainty, the concept received a zero. The net-value for each concept was calculated by adding all plus and minus, and with that each got a ranking. If two or more concepts received the same number of points, they received the same ranking.

There were a total of three iterations using Pugh-matrices. For the first iteration, the original manifold was chosen as reference. The reference was then changed for the second respectively third iteration, this is to get some variation on the reference to assure a fair comparison. After the three iterations, the ranking order for each iteration was summed and a final ranking for all iteration gave the resulting remaining concepts.

3.4 First design-phase

The winners from the concept evaluation were designed in Creo Parametric to be able to simulate them using CFD. Two concepts were designed in the first design-phase, the NACA concept and the existing manifold but with a vane. The choice of the concepts that were first modeled was driven primarily by the ease of modeling the desired geometry, aiming to reuse as many existing components as possible while still improving the system performance. To gain a quick understanding of the effects of local geometry changes, such as altering a particular bend shape, steady state simulations of small parts of the inlet manifold were carried out.

The CAD-program used for the design work was Creo Parametric as it is used internally by Volvo Group. A copy of the existing manifold assembly was made and saved to a separate workspace to allow changes to it without corrupting any other files. The part of the assembly that was re-designed was the main pipe before the plenum. This method was chosen because it appeared the most effective to make quick changes that could be carried out within the time frame of the thesis. This approach was also in accordance with the chosen incremental design strategy, changing a single component while retaining the other parts of the system.

All geometry operations that weren't desired when simulating, such as all extra operations for the mould-adaptations, cable-management and unnecessary fillets, were suppressed in the simulated geometry. This was done to ease the making of changes to the different parts in the assembly without operations intervening with each other and causing the file not to compile. All holes and fixations, for example the secondary pipes connection to the plenum and the rest of the pipe continuing to the intercooler was not changed from the original design. This to be able to introduce new designs and make them still fit with the rest of the manifold, this is the case for all designs that were made in Creo PTC.

3.5 Simulation with CFD (steady state)

To test and refine the screened design concepts they were first evaluated in a steady-state CFD simulation. The program that was used for simulations in 3D was Siemens STAR CCM+. These were done on Volvo Groups computation cluster, but within the graphical interface partition as the calculations weren't considered demanding in terms of computing power. A simplified simulation was carried out on the particular length of the primary pipe entering the plenum, focusing on a quick and informative comparison study of how the bend geometry affects the pressure drop and flow distribution in the outlet. During the steady state simulations, the designs were iterated with the feedback received from the simulation results.

3.5.1 Pre-simulation work with ANSA

Before importing the CAD-part from Creo into STAR-CCM+, the geometry needs to be processed to ensure that all surfaces align and connect properly, making sure that the geometry is sealed to be able to perform a CFD analysis on it. It is also necessary to extract only the relevant geometry, in this case the volume that is occupied by the air within the manifold. This is done in the software Beta CAE ANSA, by importing a step file from Creo Parametric of the corresponding part.

In ANSA, the surfaces of the part are repaired through a variety of operations. There are different types of errors that can be fixed within ANSA. For example, red lines indicate surfaces or edges that aren't connected which are fixed by stitching edges or lines together with for example the tool "merge surfaces" or "paste cons". Different selecting operations were used to enable isolation of the inner surfaces of the part, allowing extraction of the fluid volume relevant for the simulation.

One other important tool in ANSA is the possibility to name different surfaces and group them together in part ID's (PIDs). This assisted the workflow as the part was later imported into STAR-CCM+ and had all the correct surfaces grouped together which made them easy to select and distinguish.

Before exporting the part as a surface mesh, it had to be generated and a geometry check was carried out to ensure that all surfaces computed properly and the geometry was enclosed. Finally, the ANSA-file was exported as an stl surface mesh which could be directly imported into STAR-CCM+.

3.5.2 Simulation Setup

After the pre-processing work in ANSA, the part was imported into STAR-CCM+ into a new simulation. From this geometry one region for each part surface was created, where these regions are the ones that are used during the simulation and the imported geometry part is only used for extracting the geometrical data.

Every surface is connected to the corresponding PID that was created earlier, for example the surface of the primary pipe is one PID which made it easy to apply a suitable region to it. The imported part in the steady-state simulations was only the primary pipe before the plenum.

The region with connecting to the intercooler housing was set as a mass flow inlet and the surface connecting to the plenum set as pressure outlet. All other surfaces are automatically set as wall boundaries. These assumptions allowed for a quickly developing velocity field, while also enabling the usage of boundary conditions from 1-D simulations without assuming a given pressure drop over the simulated geometry. For the inlet mass flow an approximate value was used from the GT-Power model with the engine running at 1500RPM and full load. For the outlet pressure a similar strategy was used, using a cycle-average value of the six cylinder inlet pressures as the boundary condition.

A mesh operation was applied on the created regions, using a polyhedral mesh with prism layer meshing at the wall boundaries. Settings such as base size, max Tet-size and prism layers were tweaked to achieve a mesh that was deemed to accurately recreate relevant flow phenomena. The steady-state simulation allowed for a smaller base size of the cells as compared with the later full transient analysis, due to a much smaller usage of computational power. A volume mesh was applied to the whole main region, where a mesh scene was used to check the mesh visually along with a derived plane to see a cross section of how the mesh looked inside the pipe section. No refinement study was conducted at this stage of the analysis, therefore the $y+$ was not known and a all $y+$ wall treatment approach was used for convenience.

A physics continua was created and relevant physics models were selected that would be used in the simulation. Notably, the used models were steady state, Reynolds Averaged Navier Stokes, ideal gas and k-omega turbulence with all $y+$ wall treatment to accurately represent the physics without additionally studying the mesh refinement.

3.5.3 Running the simulation

A power on demand key (POD-key) was used to run the simulations in STAR-CCM+, both serially on the graphics interface and on the computation cluster. All designs were simulated by first initializing and the running the simulation, one separate sim-file for each design. These steady-state simulations were run locally on the GUI node of the computation cluster with a serial connection because they were not considered demanding in terms of computing power. During the simulation, different scenes were used to visualize the flow. One scalar scene with a derived cross-section plane to visualize the flow inside the pipe was used, with another scalar scene showing the velocity distribution in the outlet entering the main plenum. Different scalars can be selected, the one that was used in this case was velocity magnitude (m/s) to visualize the velocity of the gas in the design. A blue, red and yellow color map was used to visualize the different velocities and auto range on the scalar field was initially used for the value of the velocity. The simulation ran for 550 iterations until the residuals were considered periodical, which was chosen as a point of sufficient convergence.

3.5.4 Collecting the data

For the steady-state simulations it was deemed sufficient to capture a still image of the velocity field from the last iteration in order to gain a visual understanding of the flow behaviour.

Additionally, the pressure drop across the studied pipe section was calculated through a monitor. The monitor was then used in a statistics report that calculated the average pressure drop over the last 100 iterations of the simulations, which helped eliminate fluctuations from the obtained value.

3.6 Second screening and design-phase

The steady-state evaluations were followed by a second concept screening process. Even though the steady-state simulation only gives a small and simplified understanding of how a concept performs, the results from it were used as basis for the screening. This along with considerations of the available time-frame and the amount of work that all concepts required. This meant that concepts were rejected both on the basis of performance and the work that the development of the concept would require.

From the results of the steady-state simulations and the second screening process, several re-designs were implemented and new concept combinations were formed to be evaluated further. These designs now considered the whole manifold, from the intercooler exit to the intake ports on the engine block. As the design work mainly focused on the primary pipe, the part was edited in a separate file to focus on that specific part. For solutions involving two or more components, for example the primary pipe and the plenum, the changes were made directly inside the assembly but by activating the part that was being edited separately.

3.7 Simulation with CFD (full transient)

To gain a better understanding of the dynamic gas flow phenomena within the inlet manifold, a full transient CFD simulation was employed. This simulation attempted to accurately replicate the effects of moving valves and the pressure pulses that follow as an effect of the valves opening and closing.

For the full transient simulations, a new method was developed using an overset mesh approach. This was done to avoid computationally demanding re-meshing when simulating the valve movement improving the simulation's efficiency. Transient boundary conditions were also used to simulate real engine behaviour with fluctuating inlet and outlet pressures, including the pulses created during the opening and closing of the valves. The simulated fluid domain contained the geometry from the intercooler to the combustion chamber entrance. The manifold geometry along with the engine head internals were designated as a single background region, while each overset with the corresponding valve were assigned separate regions.

3.7.1 Simulation setup

Similarly as in the steady-state simulations the geometry was first imported into ANSA, where work such as surface repair, PID assignment and geometry clean-up was carried out. Additionally, the overset regions were created at this stage utilizing ANSA's convenient modelling workflow.

Creation of the overset regions was done by adding a cylinder geometry that encapsulated each valve, with the cylinder surface protruding outside the intake channel geometry as shown in Figure 3.2. The cylinder contained the valve which would later be assigned as a wall boundary, while the outer cylinder surfaces would be assigned as overset boundaries. The overset regions were applied different PID's to distinguish these different surfaces in STAR-CCM+.

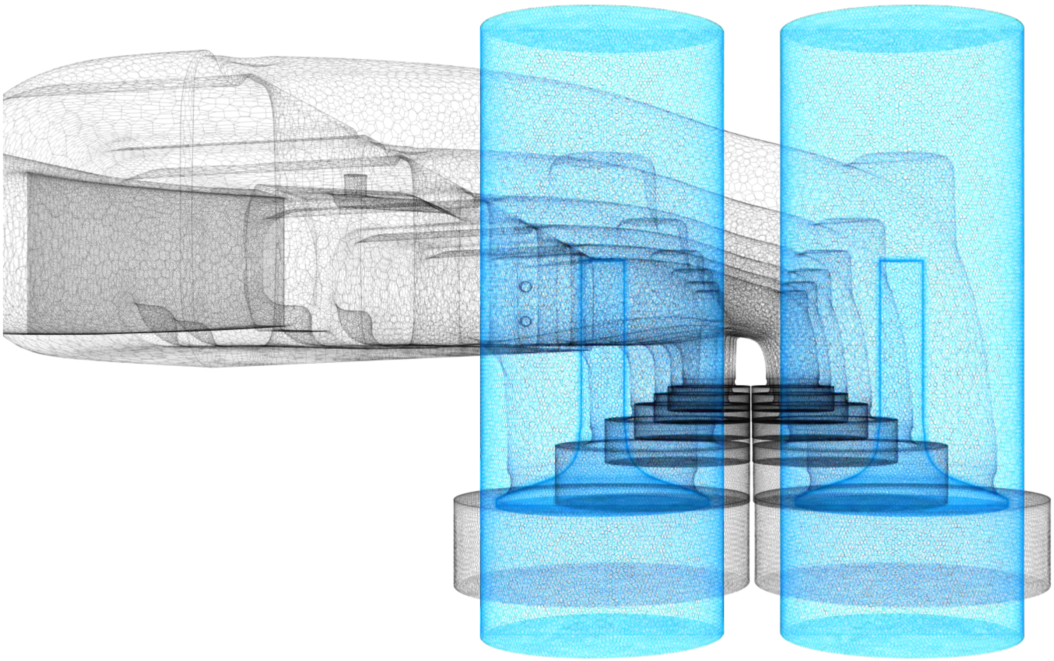

Figure 3.2: The overset interface between the background region (black) and the overset region (blue) for cylinder six.

The background region was also edited, with the valve outlets being extruded into the combustion chamber so that the overset mesh would overlap with a margin in the z-direction to ensure the overset interface would remain consistent throughout the entire movement. Simultaneously, care was taken to make sure that the vertical surfaces of the extruded outlet were far outside the overset region to avoid computational ambiguity in the later simulation. In summary, the overset constituted of three distinct surfaces, the valve along with a portion its stem and then the actual overset cylinder.

After geometry pre-processing, all parts were subsequently imported into STAR-CCM+ and a region was created for every surface. As mentioned previously, each outer cylinder surface was set as an overset mesh and the valve's two surfaces were set as walls. The surface connecting to the intercooler exit was set as a pressure inlet and the extruded outlets into the combustion chambers were set to pressure outlets. The wall connecting to the cylinder head was given a thermal specification, with a static temperature to simulate the possible temperature convection from the engine surface during operation.

When all regions were created, a overset mesh zero gap interface was created between each of the overset regions and the background region. All overset hole cutting settings were enabled for each interface using the alternate hole cutting approach, with close proximity, prism layer shrinkage and treating errors as warning enabled. The minimum gap distance was set to 1 mm for every interface and the main body's number of zero gap layers was changed to the same number of zero gap layers as for each overset.

To create the movement of the valves a translation velocity was added to each overset region. The velocities were specified by a transient input using field functions that referenced a table. Similar as in the steady state simulations, the table was populated with values from 1D simulations in GT-Power at the chosen load point and rpm. Then, different functions were created that read the table and extracted its data. These field functions were put as boundary conditions for each outlet- and inlet-region, resolving both valve velocity and the transient pressures at the system boundaries. The functions used were adjusted with the time-step variable, scaling the dynamic behaviour accordingly with the chosen time resolution of the simulation.

3.7.2 Mesh refinement

For the overset hole-cutting algorithms to work properly, the mesh of the overset and background regions needs to be of similar characteristics in terms of shape, size and prism layers. Therefore one mesh operation was created for the background region and another one for the oversets, allowing individual tuning of parameters for each subset.

For the background region or main body, a custom surface control was applied on the outlets with a target surface size relative to the parent. A custom volumetric control was also applied on all inlet ports by adding a simple box geometry that covered all ports and selecting the box to refine the volume mesh within its boundaries. A cross-sectioned representation of the mesh for one of the inlet ports with closed valves is presented in Figure 3.3 and one with open valves in Figure 3.4. An example of some of the default controls for the main body with a polyhedral mesher and prism layers is presented in Table 3.1 below.

Table 3.1: Default controls for the main body's mesh with polyhedral mesh and prism layers.

Default controls	Selected setting
Base size	0.01m
Target surface size	300% of base
Minimum surface size	10% of base
Surface curvature	36 pts/circle
Number of prism layers	14
Maximum tet size	400% of base

To achieve a similar size of elements in the overset mesh as in the main body, a custom surface control was applied to the oversets on the overset region and the valve excluding the stem, with a target surface size relative to base applied to refine the surface mesh. As mentioned before, the number of prism layers for the main body and the oversets are the same, as well as prism layer stretching to ensure that the meshes behave similarly in the interface. This was also done to lower the Y+ as the prism layers or the cells closest to the wall is the single most contributing factor to this.

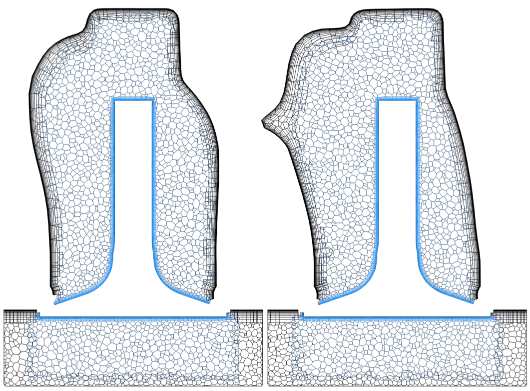

Figure 3.3: Cross-section showing the mesh of a closed inlet valve, after overset hole-cutting.

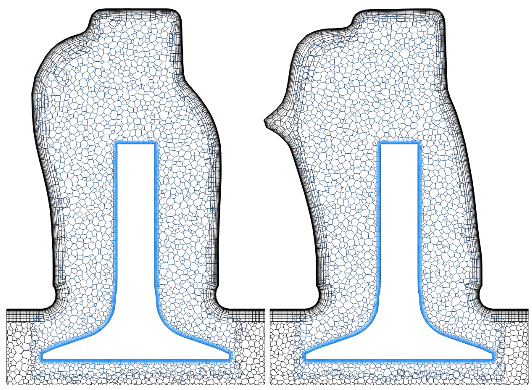

Figure 3.4: Cross-section showing the mesh of an open inlet valve with the overset region in blue.

3.7.3 Running the simulation

When initializing the simulation, the time-step was set to a lower value than the resolution of inputs from 1D and then gradually increased. This was done to achieve sufficient simulation stability upon initialization, giving the simulation model some time to adapt and develop the flow field avoiding floating point errors that terminate the simulation.

Another method that was used to get the transient simulations running was decreasing the under-relaxation factors for velocity and pressure at the start, and then gradually increasing the values once the solution stabilized. The final values used in the last iteration of the transient simulation were 0.5 for velocity and 0.15 for pressure.

Additionally, when the simulation proved difficult to get running some models were selectively disabled to help develop the initial flow-field. In the final full transient simulation used for benchmarking of the design concepts an ideal gas model was used, along with an implicit unsteady solver, k-omega turbulence modelling and a low $y+$ wall treatment model. The time-step used throughout the simulation after the initial ramp-up was $1.0^{-4}s$.

To extract the right data from the simulations, reports were set up inside STAR-CCM+ monitoring the massflow, velocity, temperature and pressure entering all six cylinders. Monitors were created out of these that print the value for each report. Subsequently, a joint plot of the mass flow was created with all six monitors together, this was done to oversee the simulation while it was running and to export the data. A specific report was setup for the cylinder head wall region to monitor possible heat transfer to the manifold. , along with the pressure plot to make sure the pressures were within a reasonable range. The massflow plot was used to extract how much flow in kg/s was induced to each cylinder and to show the distribution between the cylinders differs with design alterations.

A velocity scalar scene was used to keep track of which valves were open and to build an understanding of the general flow behaviour within the manifold. Similarly, a scalar scene displaying temperature was used to observe the heat transfer caused by the cylinder head wall. When presenting these velocity charts, it was decided to present all the designs with valve 2 completely open to give them a fair representation.

During the simulation, some scenes had an enabled "save-to-file" operation. This function saved a snapshot of the scene once triggered, which can be a determined interval of iterations. A file-system was setup to keep track of the different designs and which scene that was being saved. Notably, a scalar scene displaying velocity was used to visualize the flow and another one with a derived plane showing a cross section of all valves opening and closing. These images were later animated as a GIF-file to be able to use for presentation of the flow in the different designs. A stopping criteria was used on maximum physical time to run the simulations for a similar duration, while avoiding divergence.

The existing manifold was simulated first to provide a baseline for comparison. Engine test data and 1-D simulations were also used to verify that the developed model generated plausible results. Then, all other designed concepts were simulated one by one. A run with the original manifold was also conducted where the temperature on the cylinder head wall was set to adiabatic instead of a static temperature. This was done to see if the wall temperature hade any notable effect on the flow entering the cylinders.

3.7.4 Data Processing

The data from each mass flow plot and velocity of each valve was exported as a CSV-file to be able to extract, filter and analyze the simulation results. A python script was used to read the CSV-files and plot the data in different representations. The amount of iterations constituting a full engine cycle was computed, and used to extract flow data from exactly the 3 last full engine cycles. This approach ensured that the result wasn't skewed by any cylinder having more recorded intake vents than another. A filter-function was used in python to filter out noise from the simulation, mainly setting the flow rates for each valve to zero when the corresponding valve was fully closed.

From the recorded datasets, a bar chart was created that presented the average mass flow individually for all six cylinders over the last 3 engine cycles. The mass flow was normalized against the mean value of the dataset, aiming to only show relative changes and distribution between different cylinders. With the boundary conditions used in the simulation, computation of a pressure drop was not possible as the value was dictated by the chosen inlet and outlet pressures. Instead, the resulting mass flow was used as an indicator of the corresponding pressure drop that each design generated, allowing for a comparison between the different concepts.

To quantify the distribution, the variation between the average charging of the cylinders over the chosen amount of engine cycles was done through the calculation of the corresponding cv. The formula used is expressed in Equation 3.1, where σ represents the standard deviation, and μ denotes the mean value.

$$cv = \frac{\sigma}{\mu} \tag{3.1}$$

3.8 3D-printing of final prototype

One of the designs was chosen to be 3D-printed for testing on a flow-bench, where the best performing concept was chosen as the design to be printed. This was done both to be able to use it as a visual aid during the presentation of the project as well as the aforementioned flow testing. For this specific part, all operations including for example the mould-adaptations were corrected to the design to ensure that the 3D-printed part looked like it would have done if it was the real production part. The file was then exported as a step-file and all printing was outsourced to a division within Volvo.

4

Results

In this chapter the results are presented from the pre-study, the development of new concepts and how they performed in the conducted simulations. The results from the literature are presented in chapter 2.

4.1 Pre-Study

The pre-study in this project consisted of an analysis of competitor products, a patent search of existing solutions and finally a review of material from within Volvo Penta that contained key information about the development of the current manifold.

4.1.1 Market and competitor analysis

Scania produces an engine that runs on gas, either natural gas or biomethane. A model with 460 horsepower is called the OC13 104 460 hp. The possible configurations are 9- or 13 liter with a six cylinder In-line configuration. It has the same firing order as Pentas G17, but is intended for a different application since Scania's is for a truck and the G17 is for power generation. By visually examining the inlet manifold for their engine via one of their CAD-drawings on their official sales website, it can be seen that they use a plenum with short individual runners. The top of the plenum is below the valve cover and the runners are shaped with turning downwards from the plenum connecting to the inlet ports, doing nearly two 90 degree turns in doing so.

Another competitor for Penta is Cummins, who have several engines for power generation applications that run on natural gas. One that is comparable to the G17 in output power is the GTA38 Lean Burn Gas Series. It is a in-line six cylinder engine with a displacement of 38 liters and it has a standby power of 548-851 kVA. The plenum design is a big cube-shape with short individual runners, and the air enters from above the cylinders.

Zeppelin CAT is also a competitor for Penta. They have a wide range of products offering genset technology, but one similar to the G17 is their GC137-12. It is an in-line six cylinder engine with a displacement of 29 liters and a standby power of 500 kVA. Their manifold design is similar to Scania's with a plenum with air entering from above into short individual runners.

4.1.2 Patent search

In this section, some of the most relevant patents found during the patent search are presented.

One such finding from the patent search is a casting core from 1982 for an intake manifold which is for an in-line six cylinder engine. It has an integral core segment which forms the central plenum that expands via individual runners to the engine. It has a design in which the individual intake runners have the same length, a technique for making the distribution of air equal to all cylinders. The patent is filed by the company Bayerische Motoren Werke AG (BMW) and is an example of a solution with individual runners with equal length and a centred plenum segment [15].

A patent with a plenum that has an entering of air to the side was found, instead of a central inlet. It is for an in-line engine with three cylinders, but the principle can be used for a six cylinder engine as well. This solution has equal length runners, but with the air entering from the side of the plenum at an angle where the gas throttle is placed. Where the air enters the plenum, in the angled turn, there is a rail in the middle of the airway that splits it in half [16].

Another patent that shows a solution with individual equal length runners and air entering from the side was found. This design also features a surge chamber, which is used for storing pressurized air so it's always available for each intake pulse. One other solution described within this patent is that it's formed by plastic friction welding, ensuring smooth inner surfaces of the wall which can improve the efficiency of the manifold. The same as in the solution above with a side inlet, the runners are not circular, rather they are more oval-shaped [17].

The following solution uses a plenum with no individual runners. Instead it has a plenum with an entering from the side with nothing inside the plenum to guide the air, only an open space. It also has some other built in functions such as an air heater for assisting cold starts, but the focus is on the shape of the plenum. The patent is a collaboration between the Chinese company Foton and a competitor to Penta, Cummins and it was filed in 2019 [18]. One other feature this solution has is a gasket the cylinder head and the plenum. The patent description does not explain its purpose but this may help with either mounting or with heat for example, but likely ensures a tight seal.

4.2 Previous CFD simulations on the G17 manifold

An internal report conducting an unsteady flow analysis on the previous intake manifold design, using a k-omega SST RANS model and moving mesh with a re-meshing model approach to simulate valve behaviour, rendered some important insights into the considerations and characteristics of the existing manifold.

- A considerable improvement in charge distribution between the cylinders was achieved by placing the plenum entrance centrally in the manifold.
- Having less sharp bends created a better overall flowrate.
- Introducing blockage geometry at the entrance of the plenum did not improve distribution, and significantly decreased the overall flowrate.

4.3 Requirements and constraints

The requirements and constraints that were produced from the literature review are presented in Table A.1. The table describes attributes/aspects of the final product and if they are considered a requirement, a desire or optional. Requirement means that the final product must fulfil it, where a desire is good if it is fulfilled because it can lead to a more competitive product with, for example, a higher value for the customer or a more cost-effective product. Optional means that it is neither positive or negative if the product fulfils that specific attribute. Pressure drop are not in the table because there isn't a fixed value for this. They are possible to measure and quantify, but since they are the main optimization-objective and a value hasn't been decided for them, they are not in the requirements-table. Some of the more extensive requirements are the space requirements, fit to the existing engine block and distribution of air between the cylinders. The space requirements describes the space constraints in x-, y- and z-direction that the manifold has. Fit to the existing engine block is a requirement because the engine has fixed measurements which will not be changed, therefore the value to decide if the requirement has been met is a yes/no. Distribution of air is decided by a yes/no with a value that depend on the improvement to the original manifold.

4.4 Evaluation of Resonance

The possibility of achieving resonance in a dual manifold configuration was investigated through a python script that employed the equations shown in Equation 2.2 and Equation 2.3. Fixed values for cross-sectional areas in the primary and secondary inlet pipes were chosen based on approximations of the values in today's manifold, after which a desired resonance frequency was determined based on the rotational speed of the engine and frequency of occurring intake events in each half-plenum. This value was used to resolve a volume of the plenum chambers, assuming that this was the biggest “free variable” that could be altered. Initial runs of the program suggested plenum volumes of 18.52l for the lowest resonance frequency, a value that would make this solution difficult to employ in practice.

Another important concern regarding the resonance effects are the amplitudes of the pressure pulses generated during the intake cycles. In the engine studied in this project, the amplitudes are regarded as relatively low when compared to smaller, for example automotive application, engines that operate at higher speeds. This suggests that the potential benefits achieved through resonance within the plenum chamber could be difficult to justify with the increase of required volume and space.

4.5 Results from concept generation

This chapter describes the different concepts that were generated, and they fall into the three main categories that are presented in theory: incremental, radical and modular. They are presented along with preliminary sketches to show what the product development process looked like. A figure from the main brainstorming session is presented in Figure 4.1 below that shows the creative process on a white-board and all the generated concepts. Where the concepts were sketched and given a working name and then split into the three different types of products.

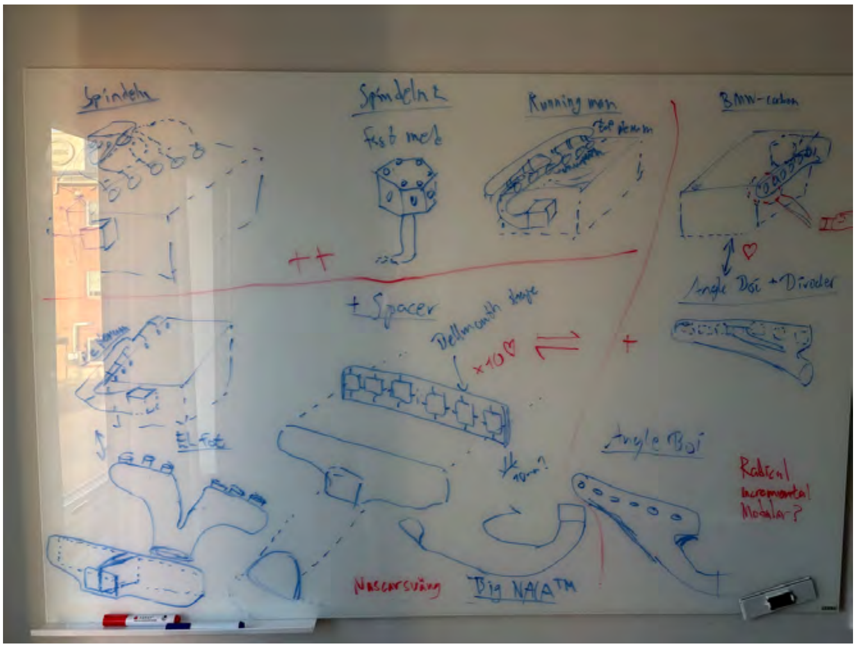

Figure 4.1: Picture of all concepts from the main brainstorming session.

4.5.1 Incremental

The following solutions are incremental solutions of today's manifold which means that they are similar to the today's manifold but with small and important performance-tweaks.

Side-plenum is a solution that is similar to today's solution, but it has individual runners added and it doesn't align with the engine-body the same way. Instead, the secondary pipe before the plenum is a 90-degree angle that leads to the plenum which is wider, then it has a central inlet just like today's solution and but with individual runners. This means that the volume of the actual plenum is the same, but it has individual runners connecting to the engine block, which means that the plenum is further away from the engine block leading to a wider solution in terms of space-aspect. The distribution was the main goal of improvement with this concept.

The foot has a central inlet like today's manifold but with a rail/vane splitting the plenum in two halves, so there are three cylinders on each side of the plenum. The pipe before the plenum is also a straight 90-degree turn to avoid as many turns as possible to decrease the risk of air releasing inside the pipe causing turbulence. This solution is with individual runners but it is also possible to have without, depending on the results from simulation. Also if distribution or pressure loss is the most important aspect. The runners are added with distribution in mind and the decrease of number of bends was done to minimize pressure loss.

The angle-plenum is similar to the original one, but with air entering from the side of the plenum instead of a central one, similarly to Volvo Penta's D17 engine. This means that the pipe is connected to the plenum with an angle which leads to a re-design in the pipes from the intercooler to the plenum-entering, along with the gas throttle, making it a more complex concept compared to the other incremental solutions. Below in Figure 4.2 is a preliminary sketch/design of what the angle-plenum could look like.

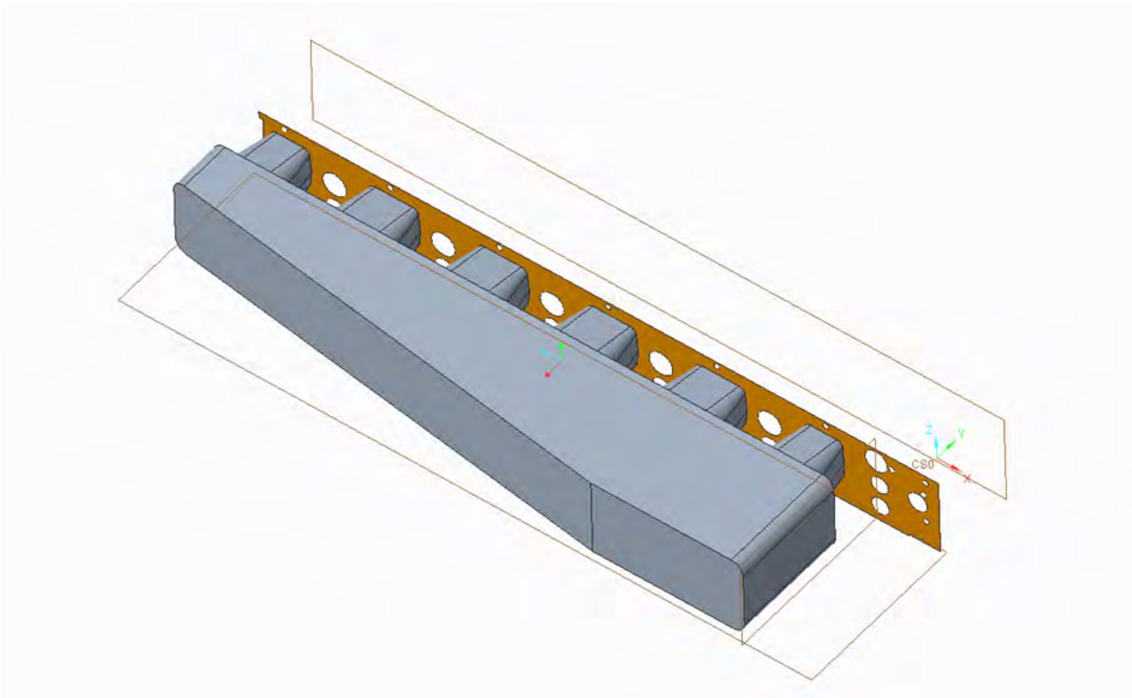

Figure 4.2: Preliminary sketch of the angle-plenum in Creo Parametric.

4.5.2 Radical

The solutions presented here are radical, which means that they are completely new-thinking compared with the previous manifold, with other ideas for solving the task and perhaps considering entirely new aspects as well.

Spindeln has a plenum with the shape of an extruded triangle, the volume of the actual plenum is much smaller than today's plenum. It has individual, equal length runners that extends from the plenum to the ports with differently shaped runners. The plenum is divided into three out-ports on either side where the runners go out to the inlet ports in the engine.

Spindeln 2 is very similar to Spindeln but the plenum has the shape of an extruded hexagon instead with one runner output from each side of the hexagon. Because of this, the runners are shaped a little bit differently than for Spindeln. It still has equal length runners but since the plenum has the shape of a hexagon the runners here has an even more complex path than Spindeln. It is inspired by the shape of an octopus.

Running man is also a concept with individual equal length runners. But the plenum is aligned with the engine block the same way as the side-plenum, but it's positioned on top of the cylinder head. Then the runners are curved downwards 180-degrees to the inlet ports. This concept along with Spindeln and Spindeln 2 are inspired by racing manifolds where it's common with for example equal length runners. In addition, the aforementioned concepts are generated with equal distribution as the most important parameter.

The free-form plenum is a intake solution similar to the angle-plenum but instead of only expanding in x-direction along the engine block, it also expands in z-direction with a more "free-form", enclosing all the ports in a single volume plenum. This solution does not have individual runners, rather the concept is designed with pressure loss in mind with the distribution less regarded.

4.5.3 Modular

With modular solutions, the manifold involves a modular solution such that the plenum is designed in several interchangeable parts in relation to the existing plenum. Two concepts that were generated are Spacer and NACA, so these are more of general design-concepts that are applicable to the other solutions on their own or in a combination.

This modular solution is the concept of a big plenum and pipe connecting to the plenum in a large NACA-bend. So the concept of a NACA-bend implemented into the whole plenum and pipe. This could for example be combined with the angle-plenum, Spacer or the foot because it can either enter from the side with an angle or with a more central inlet.

In Figure 4.3 below are some more concepts from the brainstorming including all three product categories.

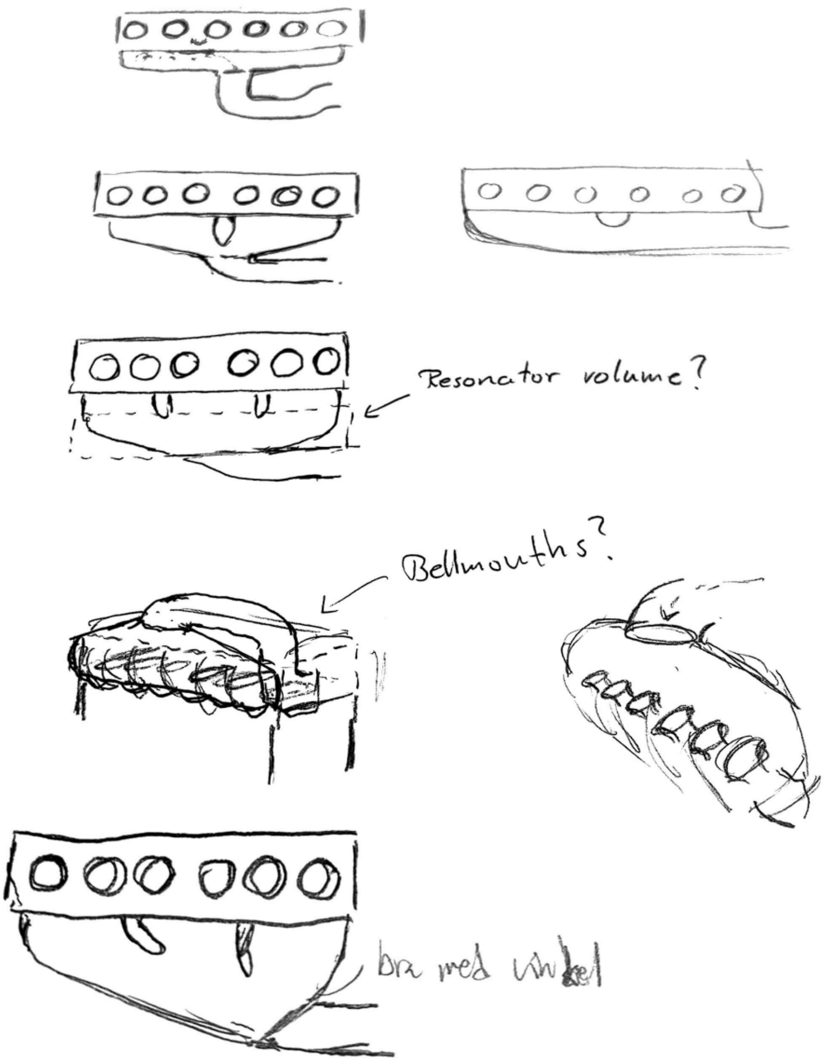

Figure 4.3: Sketched concepts from the brainstorming including the running man and side-plenum

4.6 Concept evaluation

This section presents the results from the concept evaluation after the first screening process using Pugh-matrices. Newly formulated criteria was used in the pugh-matrices to easier be able to use them for concrete evaluation of the concepts. These were retrieved from the detailed requirements and constraints that are presented in section 4.3 and modified. Some new criteria were also added.

The criteria are complexity, size, air distribution, manufacturability, pressure drop, engine response and heat insulation. Complexity describes how complex the concept is in terms of how hard it is to implement and how the air flows. Size is taken directly from the requirements table and explains the size of the whole manifold. Air distribution describes how well the concept distributes the air between the cylinders. Manufacturability describes how easy it is to manufacture the concept, this is to add the aspect of manufacturing. Another criteria is the pressure drop that describes the loss of pressure within a concept, meaning how well the air flows inside. Engine response describes how the concept contribute the engine response. Heat insulation is how well the concept keeps the air inside the manifold cool, for example by isolating from the heat generated by the engine.

4.6.1 Results from first screening

The first iteration of pugh-matrix used the existing manifold as reference, the second one used the concept “NACA” and the third one “Spindeln”. The first iteration is presented in Table 4.1 below and the two winning concepts with equal amount of points is the angle-plenum and Spacer. In second place is the NACA and the foot along with today’s manifold. The spacer is similar to the original manifold which is indicated by the amounts of zero’s it achieved and for the angle-plenum it is the same. This is mostly due to that spacer is modular, sort of a design-concept that can be applied within many of the other concepts. The radical concepts are ranked the worst, due to for example size and pressure drop.

Table 4.1: First iteration using the existing manifold as reference.

Criteria	Side-plenum	The foot	Angle-plenum	Spindeln	Spindeln 2	Running man	Free-form	Spacer	NACA	Today’s manifold
Complexity	0	0	0	-	-	-	-	0	0	Reference
Size	-	-	-	-	-	-	-	0	-	Reference
Air distribution	0	+	0	+	+	+	+	0	0	Reference
Manufacturability	0	0	0	-	-	-	-	0	0	Reference
Pressure drop	-	0	+	-	-	-	+	0	+	Reference
Engine response	-	0	+	-	-	-	-	0	0	Reference
Heat insulation	+	0	0	+	+	+	0	+	0	Reference
+	1	1	2	2	2	2	2	1	1	0
0	3	5	4	0	0	0	1	6	5	0
-	3	1	1	5	5	5	4	0	1	0
Net-value	-2	0	1	-3	-3	-3	-2	1	0	0
Rank	3	2	1	4	4	4	3	1	2	2

In Table 4.2 below is the second iteration of the pugh-matrix presented. The clear winner from this iteration is the Spacer concept. With the concepts on second place including the foot and today’s manifold similarly to the first iteration, due to for example NACA being a concept that can be applied within many of the other concepts. Along with the radical concepts ranked the worst due to for example size and complexity.

Table 4.2: Second iteration using NACA as the reference.

Criteria	Side-plenum	The foot	Angle-plenum	Spindeln	Spindeln 2	Running man	Free-form	Spacer	NACA	'Today's manifold
Complexity	0	0	0	-	-	-	-	+	Reference	0
Size	0	0	0	-	-	-	-	0	Reference	+
Air distribution	+	0	0	+	+	+	0	0	Reference	0
Manufacturability	0	0	0	-	-	-	0	0	Reference	0
Pressure drop	-	0	0	-	-	-	0	-	Reference	-
Engine response	0	0	0	-	-	-	-	0	Reference	0
Heat insulation	0	0	0	+	+	+	0	+	Reference	0
+	1	0	0	2	2	2	0	2	0	1
0	5	7	7	0	0	0	4	4	0	5
-	1	0	0	5	5	5	3	1	0	1
Net-value	0	0	0	-3	-3	-3	-3	1	0	0
Rank	2	2	2	3	3	3	3	1	2	2

The third iteration is seen in Table 4.3 below where the clear winner is the spacer concept as the two previous iterations, due to its modular nature. In the same way, the second best concepts include NACA, today's manifold and the foot. With the radical concepts ranking worst yet again.

Table 4.3: Third iteration using Spindeln as reference.

Criteria	Side-plenum	The foot	Angle-plenum	Spindeln	Spindeln 2	Running man	Free-form	Spacer	NACA	Today's manifold
Complexity	+	+	+	Reference	0	0	0	+	+	+
Size	+	+	+	Reference	0	0	0	+	+	+
Air distribution	-	-	-	Reference	0	0	0	-	-	-
Manufacturability	+	+	+	Reference	0	0	0	+	+	+
Pressure drop	-	+	+	Reference	0	0	+	0	+	+
Engine response	0	+	+	Reference	0	0	0	+	+	+
Heat insulation	0	-	-	Reference	0	0	-	+	-	-
+	3	5	5	0	0	0	1	5	5	5
0	2	0	0	0	7	7	5	1	0	0
-	2	2	2	0	0	0	1	1	2	2
Net-value	1	3	3	0	0	0	0	4	3	3
Rank	3	2	2	4	4	4	4	1	2	2

In Table 4.4 below is the final results compiled from all three iterations of Pugh-matrices. The resulting winners are Spacer, Angle-plenum, NACA, the foot and today's plenum. Out of these, angle-plenum is the only concept that has a completely new geometry and is less of an incremental solution compared to the other winners which are also incremental. The radical concepts are ranked as the worst concepts in regards to the criteria and compared to the other concepts. This is due to for example, size, complexity and pressure drop. Because the spacer concept is a modular one that is applicable to all other concepts, it was decided because of mostly the time-frame to explore other concepts, the same as for the angle-plenum. Therefore based on the gathered knowledge and time-frame, the remaining concepts are the NACA and the foot.

Table 4.4: Results from all three iterations of the Pugh-matrices.

Iteration 1 results										
Concept	**Angle-plenum**	**Spacer**	**Today's manifold**	**NACA**	**The foot**	**Side-plenum**	**Free-form**	**Spindeln**	**Spindeln 2**	**Running man**
Ranking order	1	1	2	2	2	3	3	4	4	4
Iteration 2 results										
Concept	**Spacer**	**NACA**	**'Today's manifold**	**The foot**	**Angle-plenum**	**Side-plenum**	**Spindeln**	**Spindeln 2**	**Free-form**	**Running man**
Ranking order	1	2	2	2	2	2	3	3	3	3
Iteration 3 results										
Concept	**Spacer**	**NACA**	**'Today's manifold**	**The foot**	**Angle-plenum**	**Side-plenum**	**Spindeln**	**Spindeln 2**	**Free-form**	**Running man**
Ranking order	1	2	2	2	2	3	4	4	4	4

4.7 Results of first design-phase

Under this section the results from the first design-phase are presented with initial sketches and models used in the steady state simulations.

4.7.1 Original with a vane

This design is identical with the original design but is has a guide vane at the end of the secondary pipe, a figure of the design in Creo is presented in Figure 4.4 below. The vane is in the middle and splits the secondary pipe into two pipes. It starts from where the second bend is in the pipe and stretches to before the air enters the plenum, aiming to guide the air/gas stream more effectively into the plenum. This design-tweak is an example of a design that uses inspiration from the patent search.

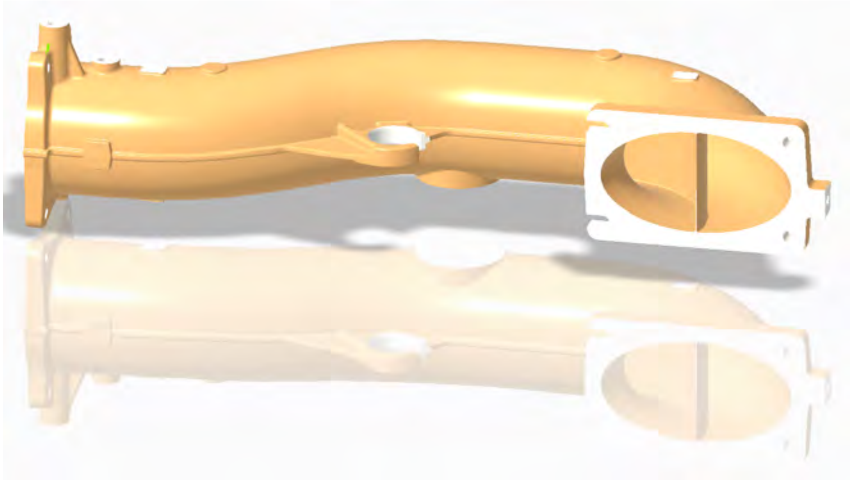

Figure 4.4: CAD of the secondary pipe for the original design in Creo PTC.

4.7.2 NACA

The NACA design is inspired by formula-1 style intake ducts, where the pipe has a bigger inner radius compared to the outer radius in a bend. This is done to decrease the air velocity at the inner bend preventing releasing of the boundary layer. This design was similar to today's manifold but the cross section defining the bend geometry has been modified, with a large radius on the inside and a smaller one on the outside. Meaning, instead of the cross-section being round, it has more of a semi oval-shape. This design of the NACA-concept is more of a minor change in relation to how the NACA was described in as a concept. This is due to the modular nature of the NACA-concept, that it can be applied within many of the concepts. But also as a result of the time-frame, as mentioned under method, today's manifold was made changes to rather than a complete new geometry.

The cross section is modified to expand gradually throughout the bend until the air enters the plenum. This is done to decrease the differences in area before the start of the bend, so some of the expansion occurs before the bend starts. This concept features more gradual transition of the wetted area, striving to minimize the possible eddy zone that is formed after the sharp bend transition. A figure of the second iteration of the NACA-design is presented in Figure 4.14.

4.8 CFD results (steady state)

Steady state simulations were conducted on iterative modifications of the secondary pipe entering the plenum, with the aim of forming a quick understanding of how pressure drop in the design can be decreased. Velocity plots of a cross section showing the interior of the secondary pipe from above were used to visualize the flow through the geometry. The key area that was focused on was the flow through the last bend entering the manifold, which introduces an abrupt change in flow direction paired with an increase in the flow cross-section. All velocity-charts are presented with a color-scale where green indicates slower and yellow up to red indicates higher velocity of the air in m/s.

4.8.1 Simulation on existing design

To form an understanding of how the flow behaves in the current design, it was the first to be simulated. The obtained pressure drop values would also later serve as a baseline for comparison with the proposed alternative designs. It was noted during the pre-study that previous simulations of the current manifold indicated a recirculating eddy zone right after the last bend of the secondary pipe, when the flow enters the plenum. The aim of the steady-state simulation was therefore to see if this could be captured without doing an analysis of the entire system.

After running the simulation for the chosen duration of 550 iterations, the computed pressure drop remained virtually unchanged over the last 100. The average value was computed over the last 100 iterations, and then recorded for later comparison. The anticipated eddy zone was clearly visible in blue during the simulation as seen in Figure 4.6, and the size of this turbulent wake could be clearly visualized when observing the cross-section of the outlet as shown in Figure 4.5.

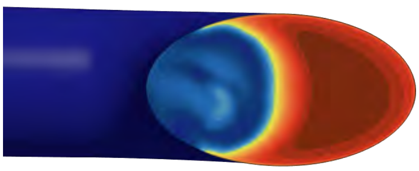

Figure 4.5: Cross-section showing the velocity entering the plenum.

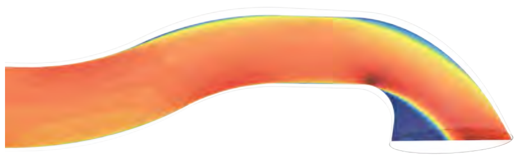

Figure 4.6: Cross-section showing velocity throughout the secondary pipe.

4.8.2 Existing manifold with a guide-vane

A guide-vane was introduced into the existing design, aiming to investigate whether the added wall friction could be outweighed by the decrease in flow-separation. It is notable from Figure 4.7 that the eddy zone has decreased in size but is still present in both channels of the split outlet. One can also observe that there is a considerable impact of the additional wall on the overall velocity distribution of the gas, which gets slowed down near the wall surfaces as seen in Figure 4.8. The average pressure loss across the last 100 iterations indicates the pressure losses are decreased by nearly 25% compared to the original design.

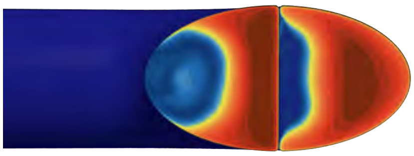

Figure 4.7: Cross-section showing the velocity entering the plenum through both channels.

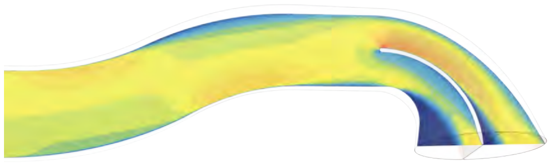

Figure 4.8: Cross-section showing velocity throughout the secondary pipe, with vane.

4.8.3 First NACA-design

The first iteration of the NACA bend was created by sweeping between two different profiles, with no gradual transition prior to the start of the bend. This design produced an average pressure drop after 550 iterations which is slightly lower than the original design, but only by about 10%. A velocity chart is presented in Figure 4.10 below. The large eddy zone was still very much present as seen in Figure 4.9, but the area that can be occupied by high-speed gas flow has slightly increased.

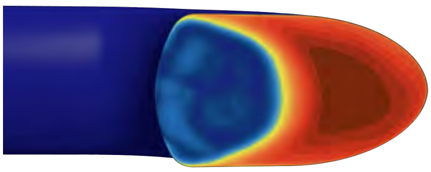

Figure 4.9: Cross-section showing the velocity entering the plenum from the NACA bend.

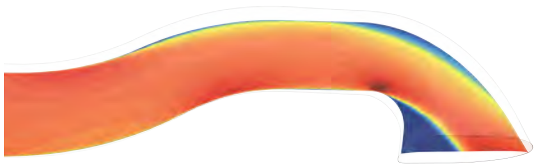

Figure 4.10: Cross-section showing velocity throughout the secondary pipe, with NACA geometry.

4.8.4 Second NACA-design

After testing the NACA concept, the geometry was modified to gradually expand before the start of the bend, increasing the cross-section diameter in the first bend definition. After running the simulation, the developed velocity field can be seen in Figure 4.11. The resulting pressure drop over the last 100 iterations implies a 33.5% decrease compared to the original manifold. The stream of gas can be visually observed in Figure 4.12 to occupy a significantly larger portion of the outlet than in the original design, and also notably more than in the first NACA iteration.

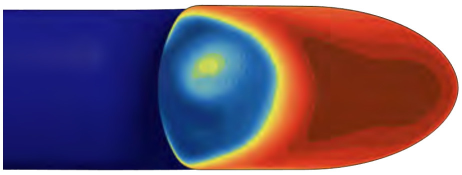

Figure 4.11: Cross-section showing the velocity entering the plenum from the gradual NACA bend.

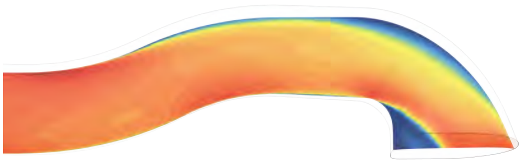

Figure 4.12: Cross-section showing velocity throughout the secondary pipe, with gradual NACA geometry.

4.8.5 Third NACA-design

For the third iteration of the NACA concept, the gradual expansion idea was tested further. The expansion was made more pronounced than in the previous iteration, but following the same basic principle. This modification didn't show the same improvements, as a significant portion of the flow separated from the outer pipe surface, which can be seen in Figure 4.13. Despite a considerable increase in pipe volume, the pressure drop was not much lower than previous iteration of the NACA concept. It can be seen that in the NACA-bend, about half of the thickness is utilized by the stream of air, and at the end of the pipe the flow uses about 60% of the pipe diameter.

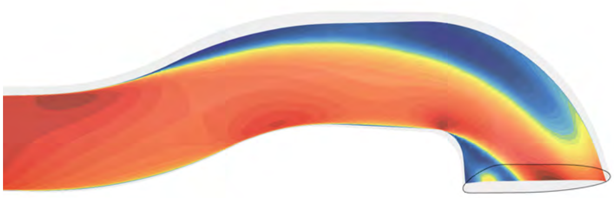

Figure 4.13: Velocity chart of the secondary pipe for the third NACA-iteration.

4.9 Results from second screening

The concepts that were left after the second screening were the the NACA concept and the foot. The promising simulation-results for the NACA design led to the Angle-plenum being disregarded because of modeling complexity and the time-frame for the project. With the Spacer being a modular solution it was determined that it can be used with any of the other winning concepts, which is discussed later under chapter 5. In addition, the second iteration of NACA was the winner and the other NACA-designs were disregarded.

4.10 Results of second design-phase

The NACA and a geometry with a vane completely separating the plenum (the foot) were the two types of concepts that passed the second screening. Therefore these were further developed during the second design-phase. The results from the design-phase are presented in the following sections. One of the designs also involves the plenum after the secondary pipe. This was done to broaden the design space without changing the complete geometry of the manifold, unlike solutions such as the Angle-plenum that was disregarded.

4.10.1 NACA

The NACA-design presented in figure Figure 4.14 below is the second iteration if the NACA concept. It features as explained in the first design-phase, a NACA-inspired bend with a larger inner radius and a smaller outer radius, with a gradual area expansion that starts before the last bend.

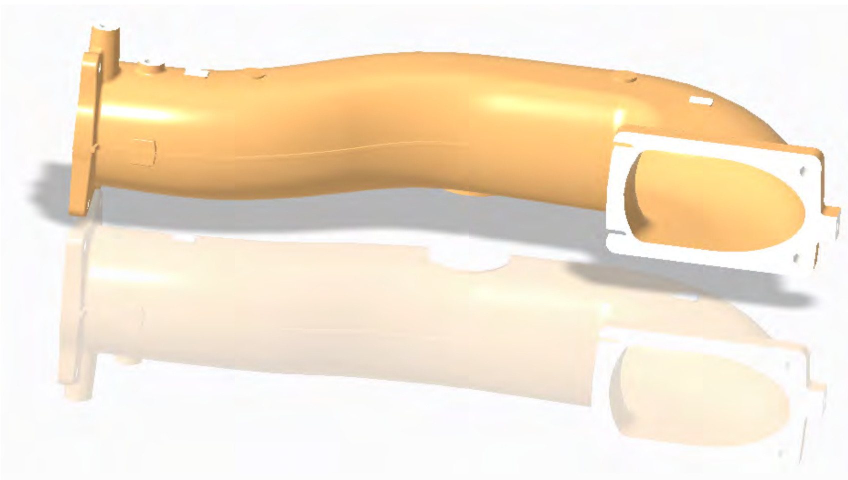

Figure 4.14: CAD of the secondary pipe for the NACA-design in Creo PTC.

4.10.2 NACA with a vane

As the vane design that was tested early on in the steady-state simulations showed very promising results, this idea was crossed with the best performing NACA geometry. The NACA with a vane is presented in figure Figure 4.15 below. It features a NACA bend exactly like the refined NACA concept, but this one has a vane with a thickness all through the pipe splitting it into two halves throughout the entire last bend. The edges on the vane inside were rounded to decrease the air-resistance.

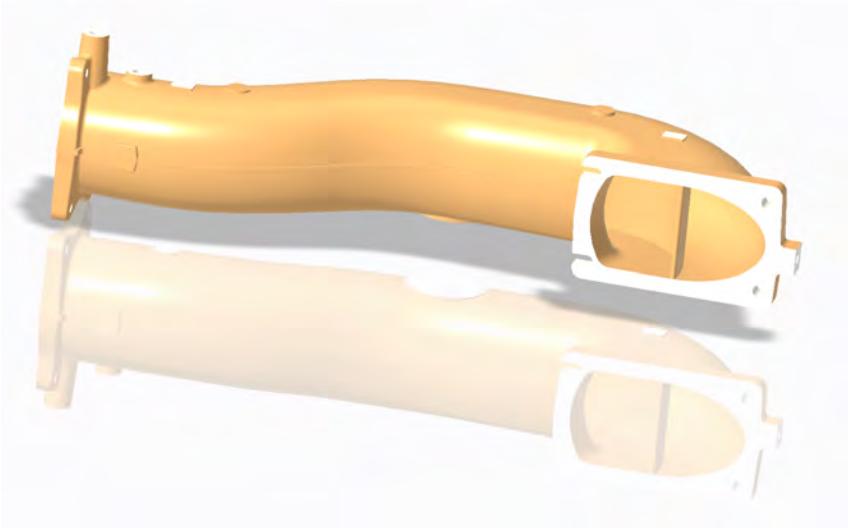

Figure 4.15: CAD of the secondary pipe for the NACA with a vane in Creo PTC.

4.10.3 The foot with a NACA-bend

The design that was given the working name "the foot" with a NACA bend is shown in figure Figure 4.16 below. It is similar to the NACA with a vane, but the vane continues up to the manifold's wall that is against the engine block, effectively dividing the plenum into two separate chambers. In other words, it's a combination between the NACA with a vane and the foot concept, attempting to combine the potential benefits of both with regards to more even flow distribution and decreased resistance.

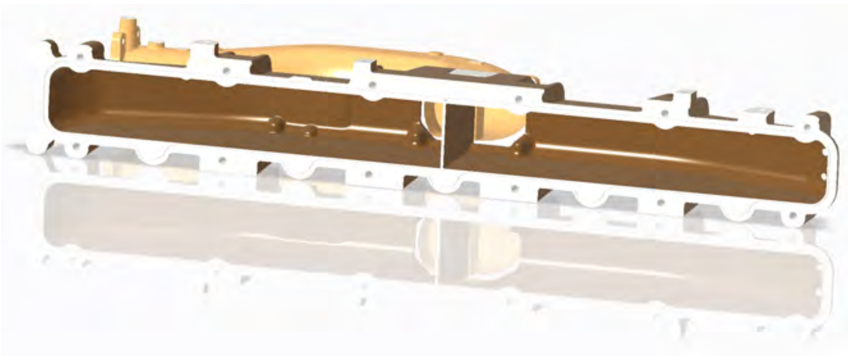

Figure 4.16: CAD of the secondary pipe and manifold for the foot with a NACA-bend in Creo PTC.

4.11 CFD results (full transient)

This chapter describes the results from the transient simulations conducted on both the existing manifold and the new designs. They are all simulated with the final developed simulation model using a moving overset mesh approach explained under chapter 3. All figures of the different designs displaying flow velocity are presented with the valves of cylinder 2 completely open to ensure a fair representation of each concept. They include the whole design-limitation space, from the intercooler outlet to the inlet ports in the engine. Notably, the throttle valve in a fully open position can be seen right before the first bend in the secondary pipe. All velocity-charts are presented with a color-scale where green indicates slower and yellow up to red indicates higher velocity of the gas mixture in m/s.

All transient simulations proved difficult to initiate, requiring up to 100 iterations at time-step as low as $10^{-6}s$, which was then ramped up to $10^{-5}s$ and finally $10^{-4}s$ after another 200-300 iterations. Throughout the ramp-up process the under relaxation factors for pressure and velocity were also kept at lower values, preventing the simulation from diverging and terminating with a floating point error. Despite this approach, the simulations would still occasionally crash at between 3000-6000 iterations, often coupled with a valve opening event. These problems were resolved by stepping the simulation with decreased under relaxation factors near the point of divergence, occasionally also decreasing the time-step until the simulation stabilized again.

To establish a baseline for comparison, the existing manifold was the first one to be tested with the unsteady simulation implementation. It was run for a total of approximately 21 000 iterations, with a simulation setup as described in chapter 3. The recorded massflows over the last 3 engine cycles, after filtering values when the corresponding valves are closed, can be seen in Figure 4.17. The average combined massflow was calculated from these values, which was considered a good representation of the total flow entering the manifold. This value was compared to the average inlet mass flow obtained with the same method in 1D simulations, where the 3D CFD value with the chosen approach was 1.39% lower.

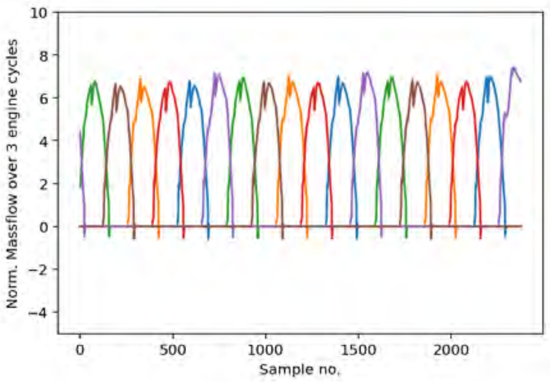

Figure 4.17: Normalized mass flows for all cylinders, over 3 engine cycles.

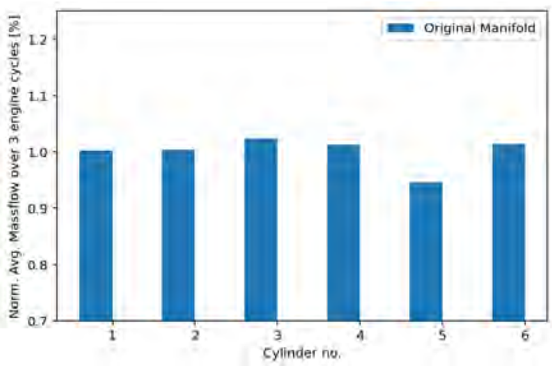

Figure 4.18: Normalized flow distribution in current manifold.

When plotting the average flow rates from each cylinder as seen in Figure 4.18, the distribution can be observed. The central cylinders, number 3 and 4, receive a slightly higher charge. The 5th cylinder experiences a significant dip in distribution, while the 6th receives nearly as much as cylinder 3. For the original manifold, the coefficient of variation was computed between the average values for all cylinders with the help of the post-processing python script. The calculated value was 0.0255, or 2.55%.

Figure 4.19: The original design with velocity represented.

It can be seen in Figure 4.19 that the velocity of the air reaches it's highest value in the inlet port, marked with dark red. Throughout the bend the values are lower, but one clearly visible feature is the wake releasing from the inner surface of the sharp bend entering the plenum.

The NACA bend design was the first modification to be tested with the new simulation model. Averages of the obtained mass flows were computed for each cylinder, and then normalized against the overall average value from the current manifold simulated in the previous step. The obtained quantities are presented in Figure 4.20 below, where the bar-chart represents the massflow in % for the NACA in relation to the today's manifold. It can be seen that this design results in a more pronounced centring of the flow distribution, with the quantity of induced air decreasing steadily when progressing outwards from the middle of the manifold. Another notable result is that the overall flow has increased, with a resulting value 4.57% higher than in the original manifold. The corresponding achieved distribution had very similar coefficient of variation, being 0.0250 or 2.5%.

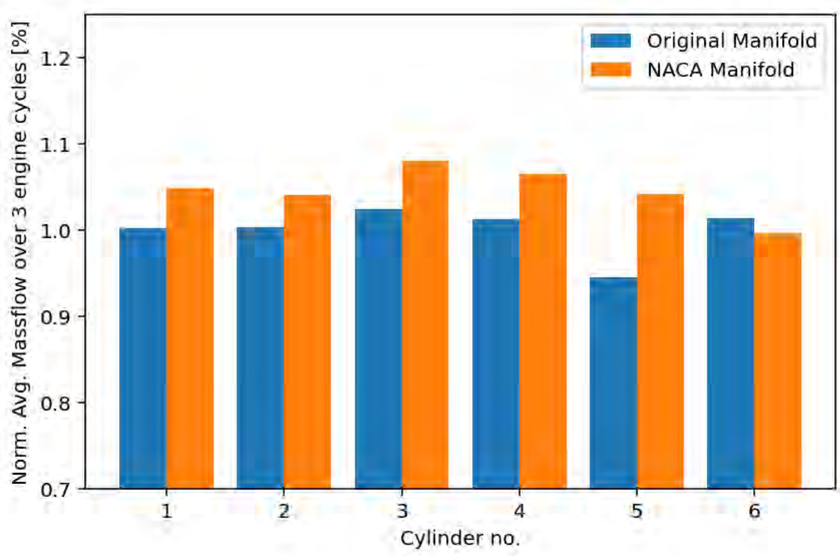

Figure 4.20: Average massflow over 3 engine cycles of the original manifold compared with the NACA design.

A velocity chart of the NACA concept is presented in Figure 4.21 below where valve 2 is completely open. The size of the wake releasing from the final bend has decreased, but a larger area of slow moving air/gas-mixture has formed on the outer side of the final turn.

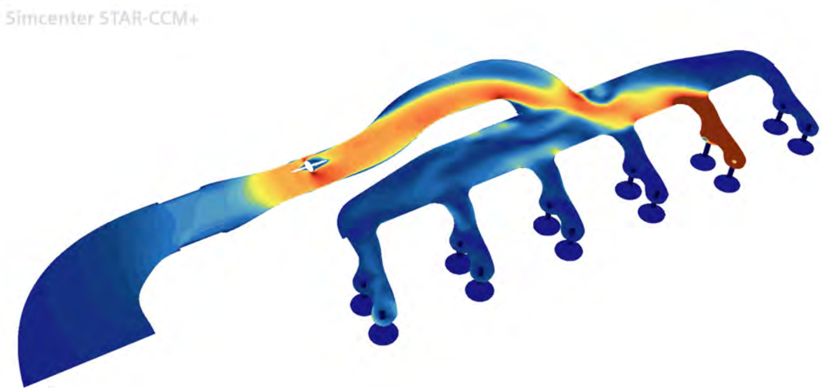

Figure 4.21: The NACA design with velocity represented.

Subsequently, in Figure 4.22, the massflow over 3 engine cycles is presented for the NACA with a vane concept compared to the original design. It can be seen that the massflow of the NACA with a vane is considerably higher. The average value was computed to be 13.0% higher than in the original design. At the same time, the coefficient of variation for the distribution was 0.0129, or 1.29%, which means a decrease of 1.26% compared to the original.

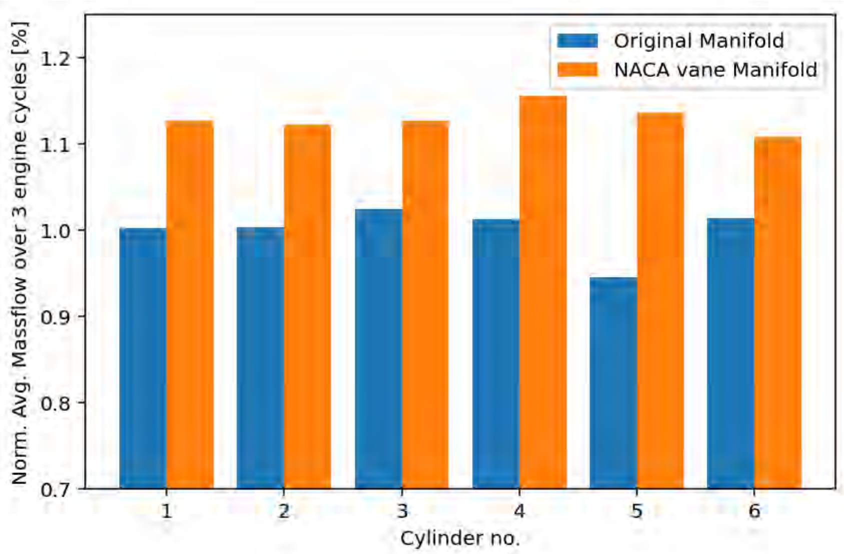

Figure 4.22: Average massflow over 3 engine cycles of the original manifold compared with the NACA with a vane.

A velocity chart of the NACA with a vane is presented in figure Figure 4.23 below. The scalar representation shows that the majority of the flow is concentrated on the one side of the vane that is closer to the cylinder 2 inlet. Notably, the overall velocity distribution throughout the secondary pipe bend has lower values than both in the original manifold and the NACA concept. The stream of air also follows the final bend more closely with a much smaller wake visible.

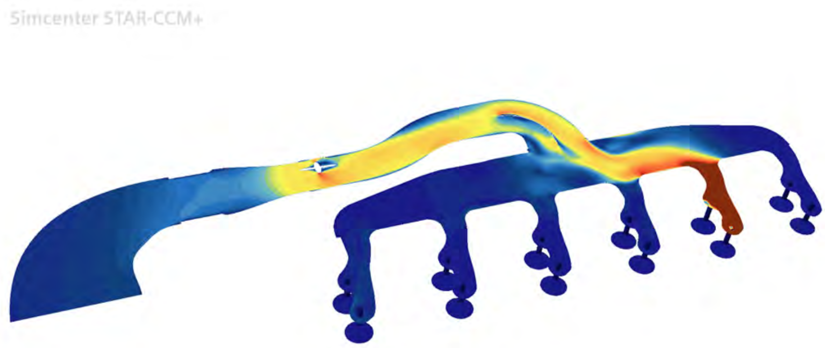

Figure 4.23: Velocity chart of NACA with a vane.

The same subset of graphs for the foot with a NACA-bend concept is presented with a velocity chart in Figure 4.25 below. The velocity has a red color in both the bend and in the inlet port indicating a high speed there while the speed before the NACA-bend and just after the NACA-bend is more moderate. The high speed flow of air/gas-mixture uses the majority of the thickness of the pipe in the final bend, developing high velocities very close to the walls. The vast majority of the flow is in the one halve of the vane that valve 2 is located in, with the other half of the plenum being virtually unused. The massflow over 3 engine cycles is presented for this design as well in Figure 4.24, showing that it is considerably lower than the original manifold with a decrease of 9.1%. The distribution was also affected, with the *cv* increasing to a value of 5.1%.

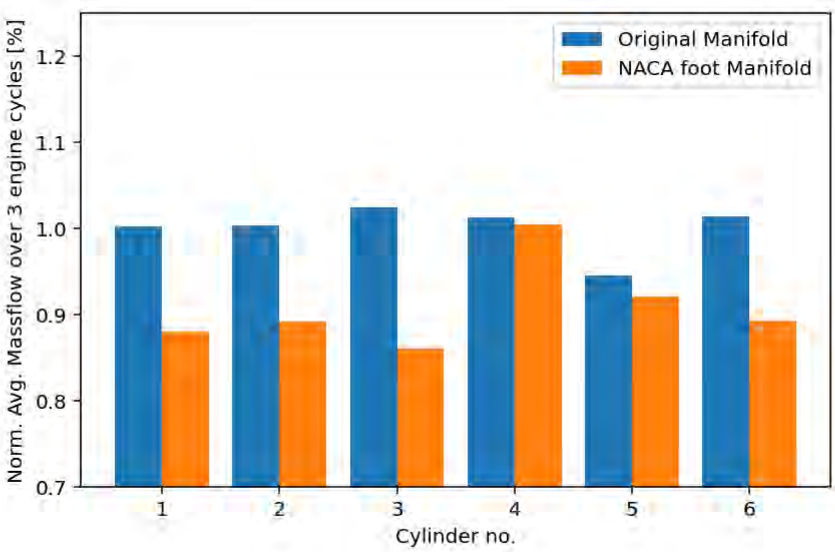

Figure 4.24: Average massflow over 3 engine cycles of the original manifold compared to the foot with a NACA-bend.

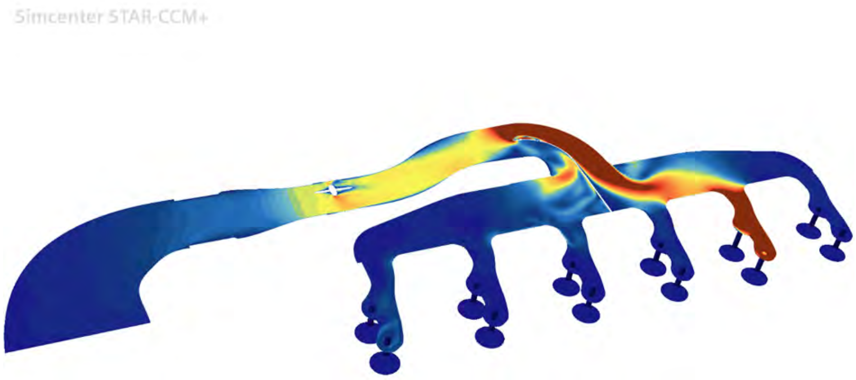

Figure 4.25: Velocity chart of the foot with a NACA-bend.

4.11.1 Temperature Analysis

To determine the effects of heat flux from the cylinder head wall, the NACA simulation was run with an adiabatic boundary condition set for that surface. The velocity distribution is shown in Figure 4.26 and can be considered virtually identical to Figure 4.21.

Figure 4.26: Velocity chart of the NACA design with adiabatic temperature as a boundary condition on the cylinder head wall with valve 2 open.

In Figure 4.27, it can be seen that with the temperature set to adiabatic, the recorded mass flow is lower than when the temperature is set to a fixed value for the NACA design, while retaining an identical distribution. The average mass flow decreased by 3.0% as compared to the simulation with activated wall temperature.

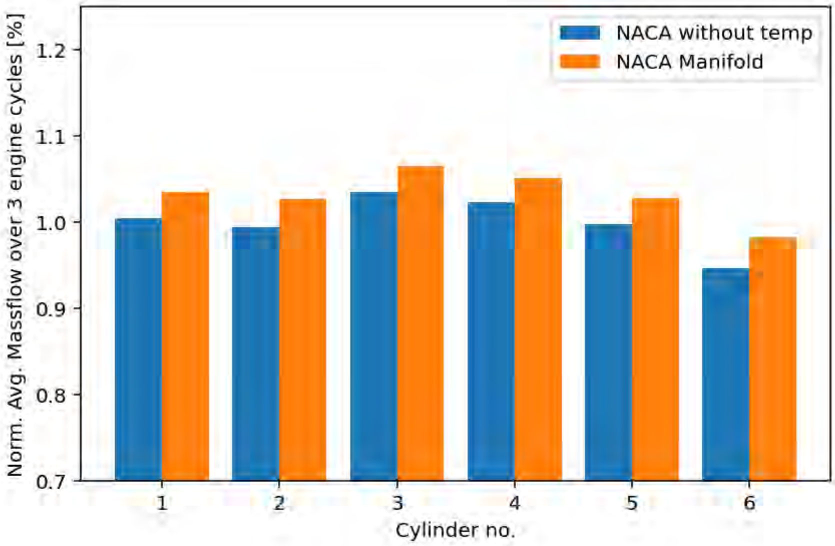

Figure 4.27: Average massflow over 3 engine cycles of the NACA design compared to NACA design with temperature set to adiabatic.

4.11.2 Mesh refinement

Attempts of refining the mesh were undertaken throughout the simulation process, with the aim of keeping wall $y+$ values at 1 or lower over the entire mesh. Decreasing the base-size of the mesh proved difficult, as the mesh took considerably longer to generate and the overset hole cutting process turned out to be very sensitive to mismatch in cell sizes. In the end, the mesh refinement approach that proved most stable was increasing the number of prism layers to a value of 14, and setting the stretch factor to 1.3.

The $y+$ of the NACA with a vane design is presented in a scalar scene below in Figure 4.28. The mesh settings for all the different designs were the same, which is the single most important factor contributing to the $y+$. As seen in Figure 4.28 the value was kept below 5 throughout most of the mesh, although some areas with higher velocities experienced slightly higher values, such as the inlet ports of the currently open valves at any point in the simulation.

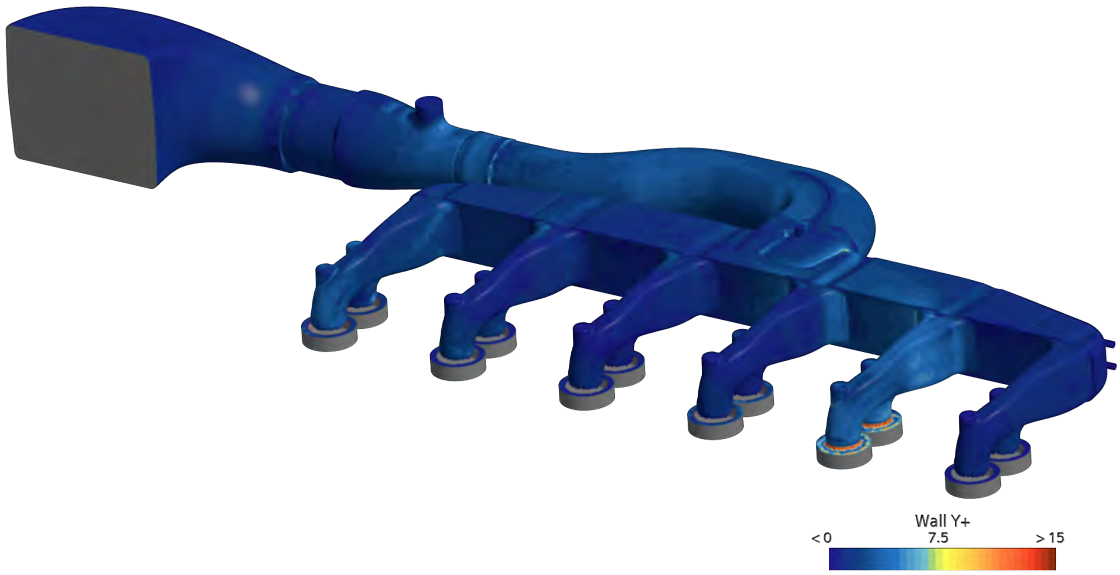

Figure 4.28: Figure showing the $y+$ of the NACA vane design with valves of cylinder 2 open.

4.11.3 Inner Iterations

An attempt was made to run the NACA with a vane simulation with an altered amount of inner iterations, aiming to reduce the simulation instability and to investigate if this parameter affects the results.

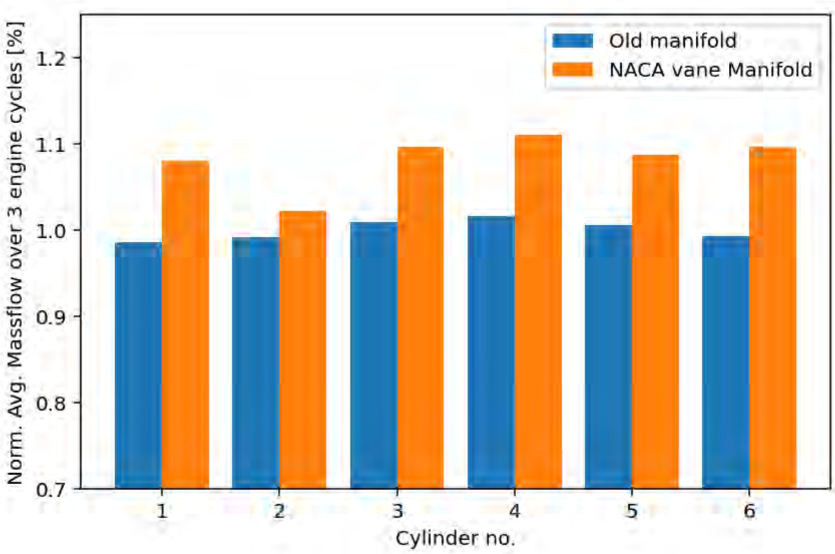

Figure 4.29: Mass flow after changing number of inner iterations

With the same aim, another run was conducted on the original manifold geometry, to determine whether the previous comparison results still stand.

The value of inner iterations was increased from the previously used 7 to 10. This caused a noticeable effect on stability, allowing a much shorter ramp-up period on lower time-step values when initiating the run, and producing consistent residuals throughout the rest of the simulation. There was also a difference in the resulting mass flow values, which can be observed in Figure 4.29 comparing the original manifold and NACA vane geometry in the new setup.

4.12 Final prototype

The final prototype was a 3D-printed model of the NACA with a vane, the design that performed the best during the simulations. It was printed in scale 1:1 and features all mould-adaptations and relevant mounting points such as screw holes, making it possible to use the prototype on a flow rig. Importantly, it featured a vane that was double the thickness of what was used in the simulations to ensure that the 3D-printed prototype was sturdy enough and printable. The material is in plastic and it fits to the real engine, a figure of it is presented in Figure 4.30 below.

Figure 4.30: Picture of the final 3D-printed prototype of the NACA with a vane.

5
Discussion

This section discusses the results gathered from the literature review, the concept development process and the simulations. In this chapter, the research questions of the project are revisited along with a comparison of the different designs.

5.1 Crucial variables

Research question: Which aspects and parameters are important to consider when improving the airflow to the engine?

An essential insight gained during the research work was that operation of turbocharged SI engines is heavily constrained by the fuels tendency to knock, spontaneously igniting in an uncontrollable manner. This phenomena causes major spikes in in-cylinder pressure and temperature, creating a high risk of component damage and failure. This means that unlike naturally aspirated (NA) engines, the performance of turbocharged designs is not equally limited by the ability to induce air, but rather the possibility of reducing knock. As a consequence, aiming for maximized volumetric efficiency may not be the correct strategy for improving the engine performance of the Volvo Penta G17. Instead of focusing on a higher volumetric efficiency, the focus of the conducted work pivoted to focus on decreased pressure drop in the system, aiming to reduce the energy lost from the compressor work of the turbocharger.

After this decision the areas identified as crucial for the engine performance were as follows:

- Reduction of pressure drop across the intake manifold.
- Minimization of variation in cylinder charging, ensuring an even distribution of the air-fuel mixture.
- Reduction of the heat transfer into the intake charge, attempting to mitigate the onset of spontaneous ignition and enabling an increase in power output.

There is also a possibility that a more controlled distribution in itself could address the knocking aspect, ensuring that the combustion in each cylinder is occurring in a more controlled manner and allowing for a better fine tuning of the engine in combination with variation of other parameters, such as ignition timing. The idea is that a more homogenous distribution of temperature caused be more equal combustion would help eliminate local hot-areas that could become starting points for knock propagation.

5.2 Suggested Design Improvements

Research question: How can an intake manifold be designed to increase engine performance with the given constraints and requirements?

The results from the transient simulations indicated that altering of the final bend exiting the secondary pipe could have significant and measurable impacts on the performance of the intake system.

An early observation from running the full simulations of the existing manifold was that the distribution is already very even, with a *cv* of only 2.55%. This result confirms the findings from the earlier conducted analysis that was used in the pre-study, showing that a centrally mounted secondary duct aids in distributing the charge evenly to all cylinders. One area that remained difficult to explain when analysing the simulation of the current manifold was why the 5th cylinder receives a notably smaller charge, while number 6 receives almost as much as number 3, as shown in Figure 4.18. A possible explanation could be that resonance effects are at play, as cylinder number 6 is located furthest away from the secondary pipe on the side where the flow has to turn sharply around the corner. It is plausible that the length of the plenum the gas travels through acts as a primary runner, creating a positively inducing resonance at the given operation point. To investigate this further, a good idea would be to run the simulation model at a different engine speed, observing whether the effect is still present.

Although the NACA concept in it's first iteration did not show any significant improvement over the baseline in the steady-state simulations, coupling it with a gradual expansion proved to have a considerable positive effect on the flow resistance. The reasoning was also that the smaller wake would allow the gas mixture to distribute more evenly throughout the manifold, something that did not manifest clearly in the unsteady simulations of the entire manifold. It did however not have a larger charging variance than the original design, albeit with a more clearly centred distribution. This design by itself could be a useful improvement allowing for a slightly less restrictive flow path with an equally good distribution.

As both the gradual NACA geometry and the guide-vane displayed a significant decrease of pressure drop in the steady-state evaluations, the decision was taken to cross these two concepts and evaluate it in the transient simulations. After simulating the NACA with a vane showed the most promising results with a large increase in terms of mass flow and a noticeably better distribution between the cylinders. In the velocity charts it could be seen that the majority of the flow of air was at one side of the vane, either at the inner radius or the outer radius. For cylinders 1-3 was the majority of the flow on the side of the vane with the outer radius while for 4-6, the majority was on the side with the inner radius. It can also be noted that the velocity for the NACA with a vane is lower all the way through the main pipe compared to a higher velocity in the regular NACA concept and the original geometry. This could mean that the air travels more efficiently inside the pipe because of the vane guiding the flow and allowing a larger portion of the exit cross-section to be used. A conclusion drawn from this is that with only a minor incremental design-tweak of the geometry large improvements in mass flow and distribution of the air/gas-mixture can be achieved. In terms of cost, the design-change is small making it comparably cheap to implement the modifications with minimal requirements of new tooling and processes for manufacturing. In other words, the performance increase in relation to cost is potentially high.

This stands in contrast to splitting the plenum in half, as in the foot with a NACA-bend. The resulting mass flow was much lower and the variance in distribution increased severely, to a value twice as high as for the original manifold. Furthermore, the velocities in the bend are higher than in the original design, which could indicate choking of the flow. The concept of splitting the plenum might still be a viable option, but the chosen implementation was likely not the right approach. As only one side of the secondary pipe could supply gas mixture to any given cylinder, the usable flow area in this section was effectively cut in half. The distribution was likely not helped by the NACA geometry which ensured that the exit of the secondary duct had different areas for each side of the plenum. In fact, it can be clearly observed in Figure 4.24 that the cylinders on the side with the larger exit radius receive a considerably larger charge. To ensure better performance of this concept, the secondary duct would need to be redesigned in order to keep the pipe cross-section closer to constant throughout the flow path, reducing the choking effect.

Another aspect from the results is that the hot wall temperature doesn't seem to have a negative impact on the flow of air/gas-mixture inside the manifold, rather the mass flow improved when the temperature of the cylinder head wall was set to a static temperature. Intuitively, the opposite should be true, because colder air inside the manifold leads to a higher density which makes it possible for more air to enter the cylinder per intake cycle. This result indicates that further investigation into this variable should be carried out, as there are many factors regarding the simulation setup that could have affected this result. It would be a good idea to further investigate the $y+$ in the area near the cylinder head wall, along with researching how STARCCM+ computes mass flows in the outlets and whether this result could be attributed to an incorrect assumption or choice of model.

On the other hand, the evaluation has shown that modular designs present a potential business case. For example, the whole plenum, with connecting pipes from intercooler to the engine has interfaces between components where it's possible to mount different plenum and pipe-designs depending on what application the engine is intended for. This allows the manifold to be optimized for its specific application. For example a gen-set engine operating on a constant rpm could have one manifold, while a harvester with varying rpm and load could use a different secondary pipe geometry or plenum design. The manifold operates as a base for interchangeable parts, almost like a platform. This makes it cost- and time effective to customize a manifold for a specific customer. Volvo Penta has niche customers and only sells the engine (powertrain), therefore this approach could be a profitable business case. Then different modules of the manifold platform can be chosen for different criteria, depending on what the required performance of the engine is. For example if distribution and performance are prioritized or if it is other constraints such as space.

From a different perspective, all radical concepts were disregarded in this project, but they may still provide promising results for another application. This is because features such as equal length runners are primarily designed for engines operating at higher rpm's, such as racing cars, with resonance effects and distribution playing a crucial role. So the application of such a concept is likely not right for gen-set technology.

Continuing the analysis of the disregarded concepts, a modular concept that was disregarded early on and which may show promising results if developed further is the angle-plenum. Its intended optimization was decreased pressure drop with maintained even distribution, and if developed further it could potentially be a high performing solution. However in the aspect of performance in relation to how easy the design-change is to implement the angle-plenum may still be disregarded later on because it requires more design-changes than for example the NACA concept. This also increases the complexity and the cost of implementing such a design. Spacer is a concept that was disregarded from the development process because the intended solution was that it could fit to any of the other concepts. The spacer may therefore be of interest by adding it to other designs that were further developed to see if it could contribute to optimize them even further through reduced heat-transfer. In addition, with a larger time frame, hybrid concepts could have been explored as well. For example a combination of the angle-plenum with a vane design to potentially also optimize the distribution.

Furthermore, the initial evaluation method that was used was Pugh-matrices that left the majority of concepts disregarded. Another tool that could have been used in addition to Pugh-matrices is for example kesselring matrices that weighs the importance of the criteria. The reasoning behind only using the Pugh-matrices as an example of a typical product development tool, is that the CFD-simulation deemed an extensive tool in itself. Continuing on the aspect of further exploring the disregarded concepts, the time-frame affected the evaluation of the concepts as the first initial screening left most of the concepts disregarded. If there was more time for the evaluation and design phase, more concepts could have given a fair chance. Just because a concept got disregarded in the initial screening, doesn't mean that the concept won't fulfill the requirements with further development.

5.3 Overset Mesh Implementation

Research question: How can a simulation method using overset mesh be implemented to simulate valve behaviour and unsteady flow?

The mesh-operations for the mesh used in the simulation used custom surface and volume controls for refinement. The custom volume control that was applied was on the inlet ports, as they interfaced with the much smaller overset domains. However, a different result may have been produced if a custom volume control was applied on the whole main body. That would have lead to a more homogenous mesh throughout the whole manifold which could have improved the accuracy of the result. A finer mesh could lead to more accurate calculations but would likely also increase the computing time. So there is a trade-off between mesh quality and data usage. But if the custom volume mesh operation would have been tested until it was optimized, it could have possibly aided in making the overset hole cutting process more stable. It is safe to conclude that the mesh refinement in the overset interface requires further investigation, in order to create a stable setup that mitigates computation errors.

A lower $y+$ was one of the goals of mesh refinement through custom volume control, but that approach proved less effective when compared to only adjusting prism layer count and stretching. The $y+$ also affects which models can be used, where the chosen model was a low $y+$ wall treatment with a k-omega turbulence model, but the result may have been different if for example a high $y+$ wall treatment or an all $y+$ wall treatment was chosen. On the other hand, if a different Reynold averaged turbulence model was chosen such as a k-epsilon model, the result could also vary significantly. In the end, the most important aspect is that the right turbulence model is chosen for the right mesh.

On another hand, the exploration of generative design as a tool in STARCCM+ was not thoroughly explored in this thesis because of the time-frame. However, if explored further it may be of help optimizing the inlet manifold. One method could be continuing on applying the generative design with the cost functions to the whole design volume. Another one could be to apply it to the already designed and simulated concepts to try to optimize them even further. This would potentially demand less computing power compared to putting a large empty volume as boundary condition, instead an already optimized smaller volume is set as the boundary condition.

One important aspect of the simulation to consider is that the time-step used didn't correlate with the time-step in the data imported from the 1D simulations. This chosen time-step was used to simplify the process of starting a simulation by stepwise increase of the time-step, to be able to only change the power of ten instead of changing the decimal. It is possible this could have an effect on the accuracy of the data resolution. Similarly, the number of inner iterations was set to 7, but if the simulation method had been explored and tested further with different values on the time-step and number of inner iterations, the results may also have differed. As became apparent when increasing inner iterations to 10, the resulting flow rates had a noticeable change. Importantly, the relatively small differences in distribution between the cylinders were skewed differently upon modification of the iteration number. This likely indicates that the previous simulations had not been converging sufficiently for each time-step, where the flow field could not develop quickly enough to adapt accordingly to the changes in boundary conditions and valve geometry. A suggestion for future fine-tuning of this parameter is to increase it until the residuals reach a chosen value, or until the increase no longer affects the result.

Another point of view is the under-relaxation of pressure and velocity that was done when running the simulations. The values were lower than the standard settings in a basic sim-file from STARCCM+. This did have an effect in terms of stabilizing the simulation and decreasing the risk of failure with a floating point error. Some simulated concepts were more unstable and the under-relaxation factors were adjusted accordingly. This could have an effect on the results because some concepts may have performed better as a consequence of the lower under-relaxation compared to other concepts, something that would benefit from further testing.

The thickness of the vane simulated in the unsteady model was half of the thickness used in the prototype, which was increased to make sure it would be structurally secure and manufacturable. The thickness of the vane used for simulation may therefore be unrealistically thin which could affect the results of the simulation. A thicker vane will most definitely affect the performance of the flow, and if further simulation were to be done, a more realistic dimension on the vane needs to be explored. Adding to that, the edges on both sides of the vane had a round-operation on them, but something worth exploring is whether the results would change if a chamfer or draft operation was used instead.

6 Conclusion

This master's thesis report presents a thorough investigation into what the development process for an air intake manifold looks like for a bio-gas engine. It explores relevant design-principles, the different stages of concept development and finally evaluates a novel method of modeling an intake system in CFD, simultaneously comparing the different designs.

An important observation is that knocking behaviour is a central factor in the limitation of performance in turbocharged SI engines, being the key problem that should be tackled when optimizing an air intake system. To affect knock, a good control of the flow distribution is likely the desirable strategy, where a good mixture and charging control can help extract the maximum performance from each cylinder. Despite the importance of knock, a reduction of pressure drop is also considered desirable as it allows a reduction of lost compressor work from the compressing of the intake charge.

One central conclusion of this work is that incremental solutions are effective design-optimizations. Changes such as editing the cross-section of the geometry and adding a simple vane showed promising results. The distribution of the original manifold can already be considered very even, but with a few modifications, the pressure drop and the variation in distribution of air/gas-mixture between the cylinders can be decreased even further. The NACA vane concept has demonstrated great potential in both tackling pressure drop while maintaining a more even distribution than the original design, presenting it as worth while for further investigation and development.

Another key conclusion is that a simulation method using an approach with overset mesh for replicating moving valves is possible, and helps make the computation more efficient than other approaches by completely eliminating the need for re-meshing throughout the simulation process. Although stability of the computation remains an aspect that requires further investigation, the method has shown a promising ability of replicating the complete shutting of valves, the following pulses that form in the manifold and consequently the resulting mass flows that are inducted into each cylinder.

Bibliography

[1] Wikimedia Commons, "Internal combustion piston engine," https://en.wikipedia.org/wiki/Reciprocating_engine#/media/File:Four_stroke_engine_diagram.jpg, accessed: 2026-02-12.

[2] Volvo Penta, "Power generation engine range," https://www.volvopenta.com/industrial/power-generation-engines/power-generation-engine-range/g17/, 2025, accessed: 2026-02-11.

[3] J. B. Heywood, *Internal Combustion Engine Fundamentals (second edition)*. McGraw-Hill Education, 2018.

[4] Environmental Protection Agency, "Global greenhouse gas emissions data," https://www.epa.gov/ghgemissions/global-greenhouse-gas-emissions-data, 2025, accessed: 2026-02-04.

[5] Volvo Penta, "About Volvo Penta," https://www.volvopenta.com/about-us/, 2025, accessed: 2026-02-04.

[6] R. P. DE Winterbone, *Design Techniques for Engine Manifolds*. Professional Engineering Publishing Limited, 1999.

[7] I. E. Idelchik, *Handbook of Hydraulic Resistance*. Springer, 1986.

[8] e. a. Bengt Andersson, Ronnie Andersson, *Computational Fluid Dynamics for Engineers*. Internal Chalmers version, 2018.

[9] T. Petra, "Description of the overset mesh approach in esi version of openfoam. in proceedings of cfd with opensource software," 12 2019, edited by Nilsson. H.

[10] S. C. Yu. Yabai, Chen. Lingshan, "The Optimization Analysis of Diesel Engine Intake Manifold based on UG and FLUENT," *International Journal of Research in Engineering and Science (IJRES)*, 2016.

[11] M. Cevitz, "Intake plenum volume and its influence on the engine performance, cyclic variability and emissions," *Science Direct*, 2005.

[12] K. T. Ulrich, *Product design and development*. New York : McGraw-Hill Education, 2020.

[13] E. Ries, *The lean startup*. Penguin Business, 2019.

[14] R. M. Henderson and K. B. Clark, “Architectural innovation: The reconfiguration of existing product technologies and the failure of established firms,” *Administrative Science Quarterly*, vol. 35, pp. 9 – 30, 03 1990, accessed: 2025-05-06.

[15] G. J. H. H. S. K. W. REINHARD, “Casting core for an intake pipe assembly for an internal combustion engine,” *Espacenet*, no. US4328854A, 1982, accessed: 2025-02-25.

[16] K. M. B. F. G. T. LLC, “Intake manifold,” *Espacenet*, no. US2014216387A1, 2014, accessed: 2025-02-24.

[17] T. H. A. I. M. C. L. L. DEXIN, “A pressure boost direct injection engine plastic inlet manifold,” *Espacenet*, no. CN207847824U, 2018, accessed: 2025-02-24.

[18] G. H. T. G. L. ZHIJUAN, “Intake manifold,” *Espacenet*, no. CN211692672U, 2019, accessed: 2025-02-25.

A

Appendix 1

Table A.1: Requirements and constraints

Requirement num.	Attribute/descriptio	Value	R/D/O	Justification	Evaluation Method	Reference
1	Maximum height of manifold	Below valve cover	Requirement	Space constraint	Measure CAD, fit to existing engine IRL	Engine enclosure
2	Maximum width of manifold	Within +10 cm of flywheel bell housing	Requirement	Space constraint	Measure CAD, fit to existing engine IRL	Engine enclosure
3	Maximum depth of manifold	Above centrifugal separator	Requirement	Space constraint	Measure CAD, fit to existing engine IRL	Engine enclosure
4	Maximum length of manifold	Within the engine block's length	Requirement	Space constraint	Measure CAD, fit to existing engine IRL	Engine enclosure
5	Withstand the boost pressure inside manifold	5 bar	Requirement	For the manifold not to explode, strength and safety aspects	FEM calculations, material choice	The manifold from D17 and G17
6	Able to manufacture final product with sand casting	Yes/No	Requirement or desire	Cost-effective; manufacturing method is not the main objective	Evaluate final designs	Existing sand-casts, structural designs of existing manifolds
7	Heat protection from the temperature of the engine block	Yes/No	Requirement	So that the charge air does not get too hot	Temperature simulations, possibly IRL validation	Temperature of current charge air through test data
8	Standard deviation of distribution between cylinders	Yes/No	Requirement	Important for each cylinder to receive equal air or gas mixture	Measure in simulations	Previous and updated simulations on G17 manifold
9	Keep existing gas-throttle	Yes/No	Requirement	Design constraint to use existing component	Check if retained	From G17
10	New intercooler housing	Yes/No	Desire	To be able to adjust it depending on application and modular design	Check if retained	Redesign from G17
11	Modular design	Yes/No	Desire	Modular design with the possibility to build the manifold with different pipes and plenums for different applications	Check if modules can be designed and attached	If possible to design and attach different modules to the manifold
12	Water drainage	Yes/No	Desire	Drain and/or trap water created through condensation so it does not enter the cylinders	Check for water, corrosion, etc.	Test data and CAD designs from G17
13	Fit to existing engine block	Yes/No	Requirement	Fit to existing screw-holes on the engine block; design constraint	Check with CAD designs	CAD designs of G17
14	Integrated mounts for electronics etc. as well as adaptations for casting	Yes/No	Desire	Integrated mounts for possible electronics and pipes interacting with the manifold	Check with CAD designs	CAD designs of G17

Department of Mechanics and Maritime Sciences
CHALMERS UNIVERSITY OF TECHNOLOGY
Gothenburg, Sweden
www.chalmers.se

CHALMERS
UNIVERSITY OF TECHNOLOGY